SERI/RR-252-1393

February 1982

MASTER

Heat Rejection and Energy Extraction Within Solar Ponds

Yogesh Jaluria

SERI

Solar Energy Research Institute

A Division of Midwest Research Institute

1617 Cole Boulevard
Golden, Colorado 80401

Operated for the
U.S. Department of Energy
under Contract No. EG-77-C-01-4042

DISCLAIMER

Printed in the United States of America
Available from:
National Technical Information Service
U.S. Department of Commerce
5285 Port Royal Road
Springfield, VA 22161
Price:
Microfiche $3.00
Printed Copy $ 5.25

SERI/RR-252-1393
UC Category: 59c, 62

Heat Rejection and Energy Extraction Within Solar Ponds

Yogesh Jaluria

February 1982

SERI/RR--252-1393

DE82 009487

Prepared under Task No. 2700.37
WPA No. 980-81

Solar Energy Research Institute
A Division of Midwest Research Institute

1617 Cole Boulevard
Golden, Colorado 80401

Prepared for the
U.S. Department of Energy
Contract No. EG-77-C-01-4042

THIS PAGE

WAS INTENTIONALLY

LEFT BLANK

FOREWORD

This study was carried out during the summer of 1981, while the author was with the Solar Thermal Research Group at the Solar Energy Research Institute. The effort was mainly directed at the basic processes related to heat rejection to and energy extraction from salt-gradient solar ponds. The author acknowledges the financial support provided by the Solar Energy Research Institute under the Sabbatical Leave Program for University Faculty. The author also acknowledges the help and support provided by Frank Kreith, David Johnson, and Federica Zangrando during the course of this work. Ms. Zangrando worked extensively with the author and contributed to the study through various discussions and background material.

Approved for

SOLAR ENERGY RESEARCH INSTITUTE

D. H. Johnson for F. Kreith

Frank Kreith, Chief
Thermal Research Branch

Barry Butler

Barry Butler, Manager
Solar Thermal and Materials Research Division

THIS PAGE

WAS INTENTIONALLY

LEFT BLANK

SUMMARY

OBJECTIVE

This report studies the thermal and fluid flow processes underlying heat rejection to the surface layer and energy extraction from the storage zone of a salt gradient solar pond.

DISCUSSION

This report details the basic heat transfer and fluid flow mechanisms involved in the recirculating flows that arise in the surface and the storage layers. The surface layer of the pond provides a convenient medium for the energy rejection from a power plant, operating on the energy extracted from the storage zone of the pond. However, the discharge of heated water into the surface layer might disturb the operation and efficiency of the solar pond, mainly because of its effect on the gradient zone. In addition, it might cause an excessive increase in the temperature and, consequently, in the evaporation at the surface. Similarly, energy extraction from the storage zone by means of a recirculating flow disturbs the gradient zone, thus lowering the temperature attained in the storage layer. It is, therefore, considerably important to determine the effect of these recirculating flows on the performance of the solar pond in terms of the disturbance to the gradient layer and the resulting temperature distribution in the pond.

After investigating available information and finding very little work on these flow problems, effort was directed at fundamental and applied studies that may be related to certain aspects of the flows. The extensive work done on heat rejection from power plants to natural water bodies, such as lakes and rivers, was used to provide information on the surface heat transfer mechanisms and on the basic features of the flow. The work on jets, particularly surface jets, and on mixed convection flows in enclosures was employed for evaluating the flow spread and penetration. The transient and steady-state temperature distributions were considered in terms of earlier studies on thermal discharges to enclosed regions. The fundamental work on stratification and on its stability was particularly valuable in determining the effect on the gradient layer due to the flow. Simplified analytical models were considered to determine the thermal and fluid flow effects that arise.

CONCLUSIONS

The gradient layer can be maintained with a negligible effect caused by the two recirculating flows if the flows are spread over the width of the pond, a suitable diffuser height is taken to reduce the flow velocities, and the diffusers are located as far as possible from the interface with the gradient zone. The flow and thermal fields are governed by two important parameters, the Reynolds number and the Froude number, which show their effect on the flow and constraints on their values for satisfactorily operating the system. Heat rejection to the surface layer results in acceptable increases in temperature and evaporation. The end-to-end configuration for energy extraction is satisfactory for large ponds and the top-to-bottom one for small solar ponds.

Experimental modeling of the problem is also studied and the important considerations for satisfactory and accurate modeling of the processes are discussed.

TABLE OF CONTENTS

		Page
Nomenclature		xi
1.0	Introduction	1
2.0	Heat Rejection to the Surface Layer	3
	2.1 The Problem	3
	2.2 Surface Energy Exchange	6
	2.3 Interface Stability	10
	2.4 Temperature Decay and Recirculation	12
	2.5 Governing Parameters and Future Work	14
3.0	Energy Extraction from the Storage Zone	17
	3.1 The Problem	17
	3.2 Penetration of Flow into the Storage Layer	18
	3.3 Flow Recirculation	24
	3.4 Interface Stability	29
	3.5 Governing Parameters and Experimental Modeling	31
4.0	Conclusions	37
5.0	Recommendations	39
6.0	References	41

THIS PAGE

WAS INTENTIONALLY

LEFT BLANK

LIST OF FIGURES

Page

2-1 A Salt-Gradient Solar Pond 3

2-2 Flow in the Surface Layer Caused by Heat Rejection 4

2-3 Heat Rejection to Natural Water Bodies 5

2-4 Surface Energy Exchange 7

2-5 Heat Loss at the Surface of a Water Body as a Function of the Surface Temperature for Various Values of Wind Speed 9

2-6 Interface Stability 11

2-7 Temperature Distribution in One-Dimensional Horizontal Flow with Heat Loss at the Surface for Different Heat-Rejection Rates 13

2-8 Streamlines for Outflow at Various Depths 13

2-9 Transient Nondimensional Temperature Profiles in an Enclosed Water Body 14

2-10 Temperature Profiles in an Enclosed Water Body with Inflow and Outflow Located at the Top on Opposite Sides 14

3-1 Flow Configuration for Energy Extraction 17

3-2 Two-Dimensional Surface Source of Buoyant Fluid 19

3-3 Predicted Jet Thickness and Density Deficiency in Surface Horizontal Buoyant Jet for $k = 1/R = 0$ 19

3-4 Dependence of Velocity, Jet Thickness, and Temperature on Entrance Richardson Number 20

3-5 Dependence of Entrainment and Downstream Flowrate on the Froude Number Fr 21

3-6 Streamline Plot Ψ/Q 22

3-7 Two-Dimensional Horizontal Flow with Intake and Outfall on the Same Side for Various Values of the Aspect Ratio D/L of the Water Body 25

3-8 Steady-State Solution at $Gr/Re^2 = 12.3$, $Re = 50$ 26

3-9 Energy Extraction from Region with Negligible Flow 27

LIST OF FIGURES (Concluded)

Page

3-10 Trajectories of Horizontal Buoyant Submerged Jets.................. 30

3-11 Typical Trace of Exit Water Temperature............................ 32

3-12 Transient Behavior of the Temperature Profiles with Inflow and Outflow Located at the Top and Bottom, Respectively........... 33

3-13 Outflow Temperature versus Time with Inflow and Outflow Located at the Top and Bottom, Respectively....................... 34

LIST OF TABLES

Page

2-1 Summary of Results for Heat Rejection............................... 16

3-1 Summary of Results for Energy Extraction............................ 35

NOMENCLATURE

A	surface area
B	depth
Cp	specific heat
d	thickness of flow region
D/L	aspect ratio
e	energy extraction parameter
E_{s1}	solar energy absorbed in storage layer
Fr	Froude number
Gr	Grashof number
g	acceleration caused by gravity
H	surface energy loss per unit area
h	heat transfer coefficient
He	evaporative heat flux
H_{br}	back radiation
h_c	convective heat flux
h_o	heat of flow channels
H_r	total heat rejected
H_s	mean incident flux
k	thermal conductivity
L	length
P	atmospheric pressure
p	pressure
Pr	Prandtl number
P_s	partial vapor pressure (surface)
P_a	partial vapor pressure (ambient)
Q	flow rate
q	flow per unit width
q_H	heat transfer per unit area
Ra	Rayleigh number
Re	Reynolds number
Ri	Richardson number
Ri_o	entrance Richardson number
T	temperature

T_a	temperature (ambient)
T_e	equilibrium temperature
T_s	temperature (ambient)
U, u_o, U_o	velocity
V, V_o	volume of the layer
x	horizontal distance
z	vertical coordinate
α	thermal diffusivity
β	coefficient of volumetric thermal expansion
ν	kinematic viscosity
δ	withdrawal layer
ρ	fluid density
ε_H	thermal diffusivity
ΔT	temperature difference
σ	Stefan-Boltzmann constant: 5.7×10^{-8} W/m^{2}k^4
τ	time
η_T	powerplant efficiency
ψ	streamfunction
μ	coefficient of viscosity

SECTION 1.0

INTRODUCTION

This report describes the performance of a nonconvective, salt-gradient solar pond using recirculating flows for heat rejection to the surface layer and for energy extraction from the storage layer. Solar ponds act as collectors and long-term storage systems for solar energy and have considerable promise for power generation and low-temperature applications. Since the surface layer of the pond is at a temperature close to the ambient temperature, it can easily be used for heat rejection from a power plant operating on the energy extracted from the solar pond. However, the recirculating flow used for the heat-rejection process (e.g., in the condensers of the power plant) will increase the temperature of the surface layer and cause additional disturbance to the nonconvective gradient layer. Therefore, it becomes important to determine the effect such a flow would have on the performance and operation of the solar pond, particularly the effect on the gradient layer, the increase in surface temperature, and the consequent increase in surface evaporation. Also, determining the optimal distance separating the hot water inflow and the cold water outflow in the surface layer would be interesting.

Considering the use of a recirculating flow to extract energy from the storage layer also demands studying the effect this flow would have on the gradient layer. Different flow configurations could be used for energy extraction. One would be to locate the inflow and outflow ports at the opposite ends of the layer; another would be to locate both ports on the same side, one above the other. The latter, if feasible, would be particularly useful for medium- and large-sized ponds, since it would considerably reduce piping expenses and heat losses in the extraction process. However, it is important to determine the distance to which the flow penetrates before being recirculated to the outflow port. This could limit the size of the pond from which this configuration can extract energy efficiently using the full length of the storage layer. For both configurations, the basic physical parameters that govern the flow and the related thermal field in the solar pond need to be determined, particularly concerning the disturbance to the interface and the mixing of the cold entering fluid with the hot fluid of the storage zone. This should also be considered when experimentally modeling actual pond conditions and analyzing the underlying physical processes.

Heat rejection and energy extraction are treated individually despite certain similarities, since the basic concerns are quite different. The heat rejection problem is considered first, since considerable information exists on heat rejection from power plants to natural water bodies. Much of this information is directly applicable to the present problem, although there are several important differences. Some of this information can be used with modifications for the energy extraction problem as well.

Not much work has been done on the flow and thermal fields caused by energy extraction from the storage layer, and the process needs to be investigated. This report outlines some of the simplified analytical models that may be employed and presents preliminary results based on earlier studies of heat rejection to water bodies. It also gives the governing parameters and discusses the underlying physical mechanisms.

SERI

SECTION 2.0

HEAT REJECTION TO THE SURFACE LAYER

2.1 THE PROBLEM

The surface layer of a solar pond is typically 0.1 to 0.4 m deep and absorbs approximately 40% of the solar flux at the surface. The mean incident flux H_s, averaged over 24 hours, is around 200-250 W/m^2 for solar pond sites in the western United States. About 20% of this energy is absorbed in the storage zone. Figure 2-1 shows the typical depths of the three zones and the shape of the temperature profile that arises.* The temperature distribution in the gradient zone is generally nonlinear because of the nature of energy absorption in the zone. The salinity distribution is similar, giving rise to an essentially uniform salt concentration in the convective surface and storage zones. The fluid density, therefore, increases downwards in the gradient region, resulting in the desired nonconvective circumstance.

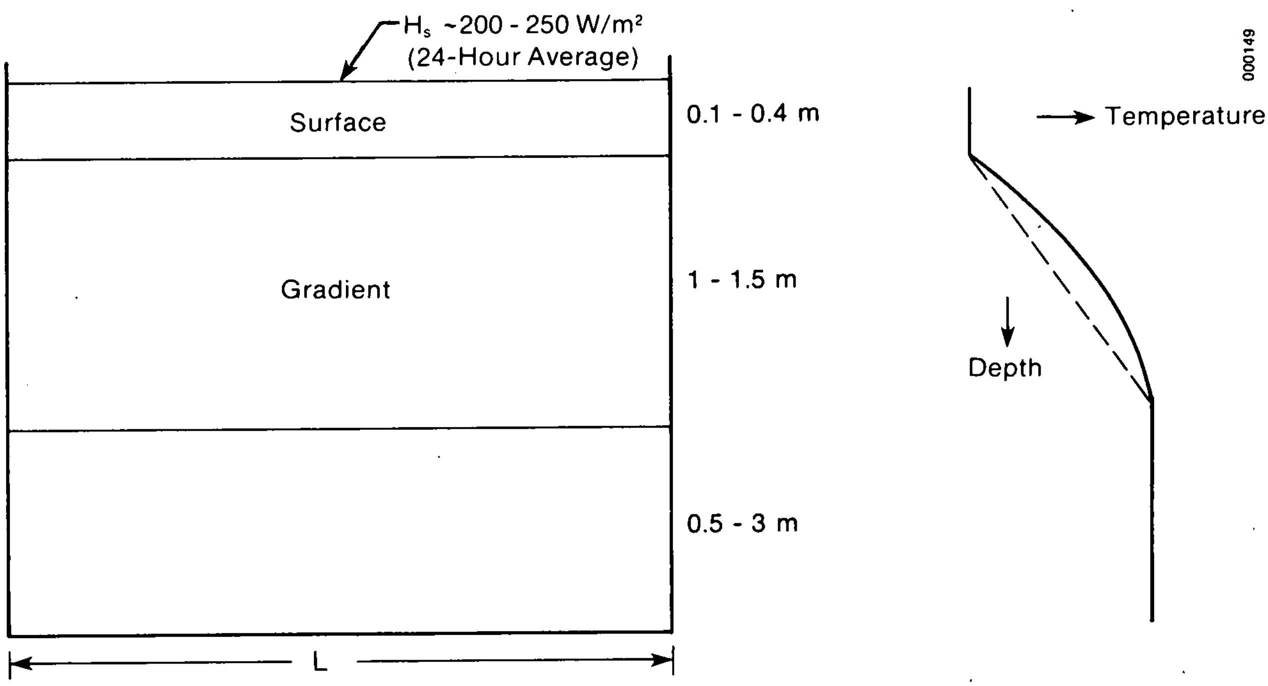

Figure 2-1. A Salt-Gradient Solar Pond

The flow field in the surface layer caused by heat rejection is qualitatively shown in Fig. 2-2. Since the entering fluid is warmer and, hence, buoyant, the flow stays mainly near the surface; the stable density distribution

*Further details on the operation of a solar pond may be obtained from Elata, Levin, and Hadar (1962), Elata and Levin (1965), Harris and Wittenberg (1979), Nielsen (1976, 1979), Tabor (1980), and Zangrando and Bryant (1977).

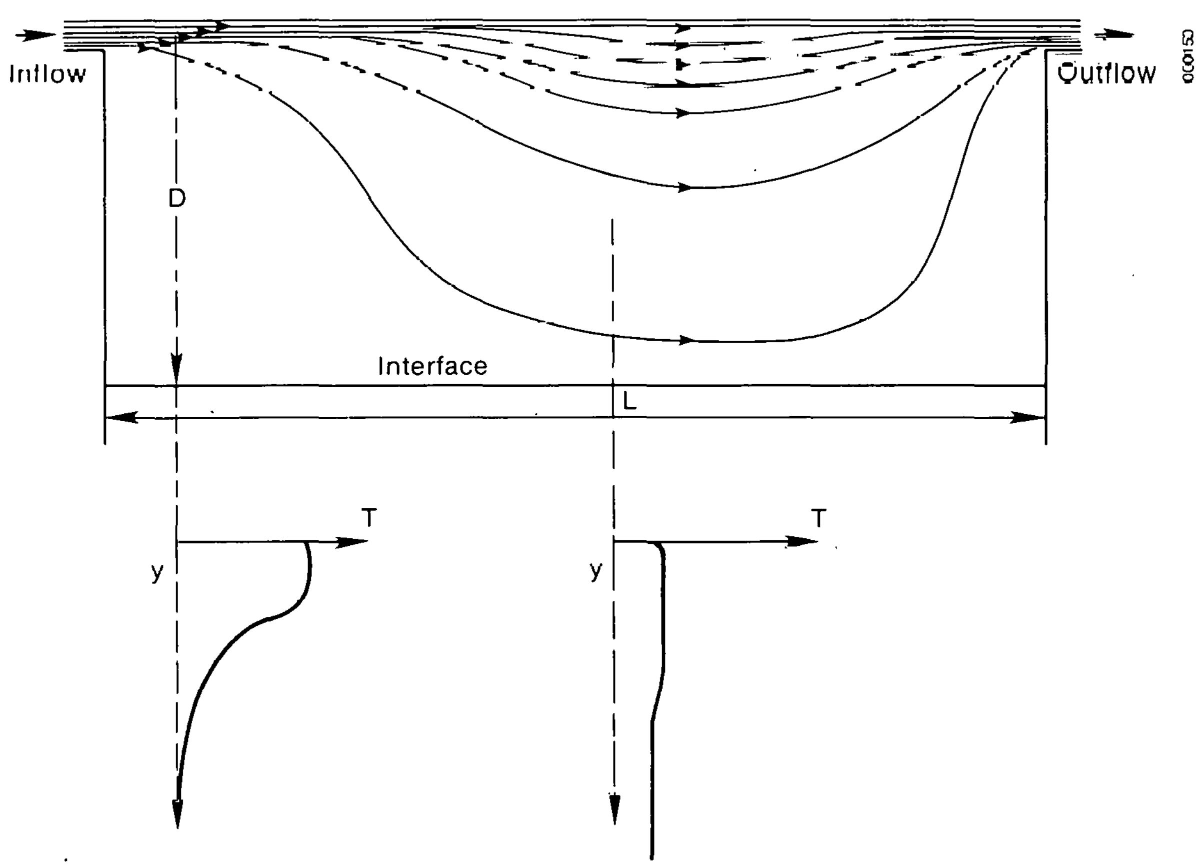

Figure 2-2. Flow in the Surface Layer Caused by Heat Rejection

restricts the downward penetration. The heated fluid loses energy to the atmosphere as it moves from the inflow to the outflow. Therefore, the problem mainly involves horizontal convection and diffusion with energy loss to ambient rather than vertical transport, which is generally a greater concern in heat rejection to natural water bodies such as the deep, stratified lakes shown in Fig. 2-3. Most studies on power plant heat rejection to water bodies discuss stratification characteristics and, in several cases, use vertical one- or two-dimensional models. Simulating the natural water body and studying the resulting thermal effect regarding the stratification cycle have been particularly interesting [see Moore and Jaluria (1972), Jirka, Abraham, and Harleman (1975), Mitry and Ozisik (1976), Spalding (1977), and Jaluria (1979)]. Since the flow is predominantly horizontal, the horizontal transport mechanisms and the surface loss have to be considered. Sehgal and Jaluria (1979) considered horizontal recirculation caused by thermal discharge into a water body, and some of their results related to this problem are discussed in Sec. 2.4.

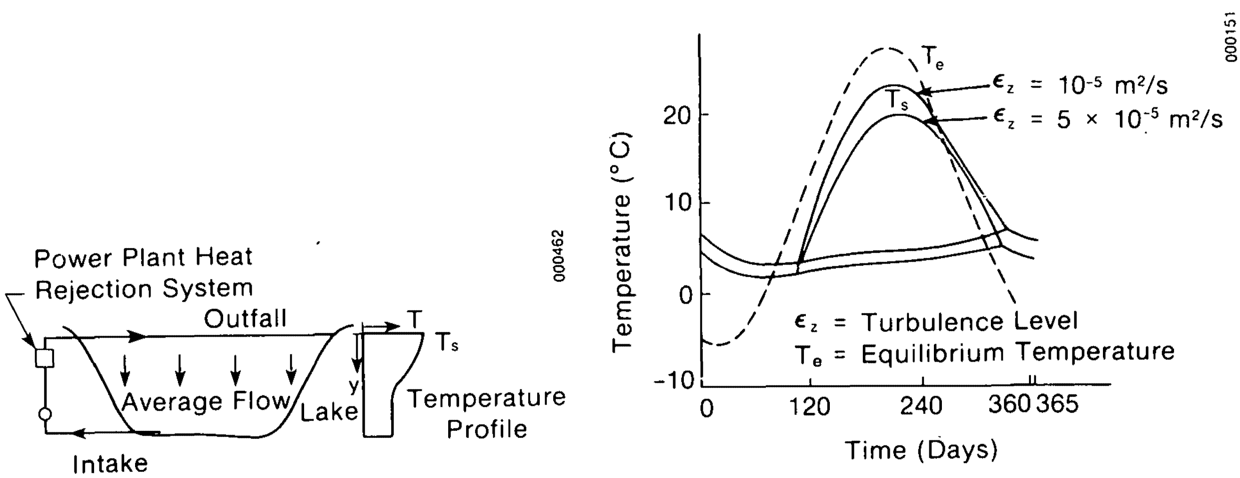

(a) Sketch of a thermal discharge system

(b) Yearly temperature cycle of a natural lake with delay in the onset of stratification

SOURCE: Jaluria 1979

Figure 2-3. Heat Rejection to Natural Water Bodies

The main concerns pertaining to heat rejection to the surface layer are:

- increase in surface temperature,
- increase in evaporation,
- increase in temperature at the outflow,
- disturbance to the interface, and
- increase in the depth of the surface layer.

These are related to the thermal field that arises in the surface layer. The increase in the surface temperature and the consequent increase in evaporation are important in evaluating the thermal impact of the rejected energy on the surface zone. If the evaporation increase is beyond acceptable limits regarding the make-up water needed, heat rejection to the surface layer will not be desirable.

The increase in the temperature at the outflow is important, since this causes an increase in the cooling water temperature for the power plant and a decrease in plant efficiency. The outflow needs to be located where the temperature increase is negligible. This will limit the size of the power plant that can be cooled by a given pond.

The disturbance to the interface and the possible increase in depth of the surface layer are important, since an increase in the surface mixed-layer depth decreases the energy reaching the storage layer and, hence, the operating temperature. Each centimeter increase in the depth of the surface layer decreases the operating temperature by about 0.5°C. Let us first consider some of the individual aspects of the problem and then determine the governing mechanisms and parameters for the general circumstance.

2.2 SURFACE ENERGY EXCHANGE

Considerable information exists on the basic physical processes concerning energy transfer at the surface. The dominant modes are solar heating, evaporation, convection, and back radiation (Fig. 2-4). Under steady-state conditions, the total energy gained from the solar flux, conduction from the gradient layer, and energy rejected by the power plant is lost by evaporation, convection, and back-radiation. In the absence of the power plant, the surface temperature is at a value (termed the equilibrium temperature) such that the net energy gained by the layer is zero at steady state. The temperature increases to a new value when energy is rejected to the layer, so additional energy is lost to the environment.

There are several, detailed studies on the surface exchange mechanism. For lakes and ponds, the results of Raphael (1962), Edinger, Duttweiler, and Geyer (1968), Hindley and Miner (1972), Ryan, Harleman, and Stolzenbach (1974), and Noble (1981) may be used. For seas and oceans, the correlations employed by Wada (1967a,b; 1968a,b) are based on detailed investigations of several workers. From Raphael (1962) the correlations for the evaporative heat flux H_e, the back radiation H_{br}, and the convective heat flux H_c are obtained as:

$$H_e = 21.7U(p_s - p_a) \quad (2\text{-}1)$$

$$H_{br} = 0.97\sigma(T_s{}^4 - \beta T_a{}^4) \quad (2\text{-}2)$$

$$H_c = (0.0041)UP(T_s - T_a) \quad (2\text{-}3)$$

where

U = wind speed in m/s;

p = partial vapor pressure in kPa;

P = atmosphere pressure in kPa;

σ = Stefan-Boltzmann constant is 5.7×10^{-8} W/m^2K^4;

T = temperature in K where subscript s is surface and subscript a, ambient;

H = heat flux in W/m^2; and

B = constant dependent on cloud cover and ambient vapor pressure.

These expressions are valid for the usual range of velocities encountered in practice. At very low velocities (less than 1 mph) natural convection becomes important and the work of Ryan, Harleman, and Stolzenbach (1974) and Shah (1981) may be used to determine the evaporative heat transfer flux. Similarly, for surface evaporation in oceans, Wada (1967a,b; 1968a,b) gives the convective heat transfer coefficient h in W/m^2K as:

$$h = 11.6(0.46 + 0.272U) \quad . \tag{2-4}$$

For evaporation, the similarity between heat and mass transfer is used to obtain the mass transfer coefficient. For example, if the wind speed is 10 km/h, the surface and ambient temperatures are 30°C, and the relative humidity is 0.2, Eq. 2-1 gives H_e as 206.2 W/m^2. Using Eq. 2-2, back radiation is 93.0 W/m^2 for a clear sky for which B = 0.8 at 30°C and 0.2 relative humidity (Raphael 1962). Convection is zero in this case. This also gives an evaporation of 8.4×10^{-5} kg/m^2-s, which amounts to 84 kg/s for a pond 1 km^2 in area. If the surface temperature is 27°C with the same ambient conditions,

000152

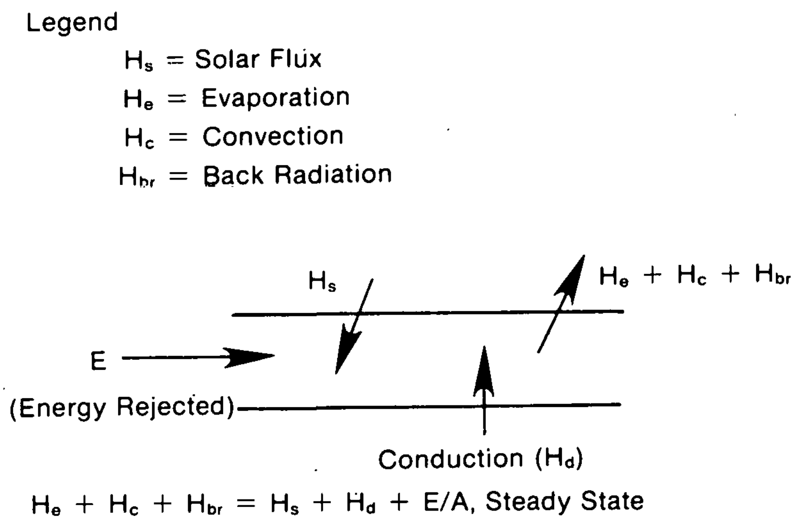

Figure 2-4. Surface Energy Exchange

H_e = 160.8 W/m^2, and evaporation from a 1-km^2 area pond is 65.5 kg/s, which corresponds to 5.6 mm/day, a value that agrees with the observations of Zangrando and Bryant (1977). Therefore, the natural evaporation increases by about 9% if the surface temperature rises by 1°C.

The surface temperature under steady-state conditions may be determined by considering an energy balance of the surface layer. If we consider the surface to be 27°C with the ambient at the conditions given above; H_e, H_{br}, and H_c are 160.8, 89.4, and -11.2 W/m^2, respectively, the last quantity being a convective gain. Therefore, the surface energy loss is 239 W/m^2 at this temperature. If the solar flux is 350 W/m^2, the energy absorbed in the surface layer, taking a 40% absorption, is 140 W/m^2.

Similarly, the heat rejected from the power plant may be determined. For a 3-MW plant with 8% thermal to electric efficiency on a 1-km^2 pond, the heat rejected is 34.5 W/m^2. Also, the heat conducted into the layer from the gradient zone may be determined. For a typical temperature gradient at the interface of 100°C/m, which is about twice the average gradient in the nonconvective zone, this gives the conduction from below as 63.7 W/m^2. Thus, the net energy loss by the surface layer is 239 - 140.0 - 34.5 - 63.7 = 0.8 W/m^2. The equilibrium surface temperature, therefore, will be slightly less than 27°C under these conditions, so the net loss by the layer is zero. This is just an example of the computational procedure. It could easily be programmed and the computer used to determine the steady-state surface temperature under specific conditions with and without heat rejection.

Figure 2-5 shows the surface heat loss as a function of the surface temperature for a natural water body. The curves are plotted for several wind speeds assuming a clear sky, a relative humidity of 0.2, a solar flux of 200 W/m^2, and an ambient temperature of 25°C. These curves are for a deep lake and the entire solar energy flux is absorbed in the water body and ultimately lost to the environment. There is no energy extraction. The temperature for zero net surface energy loss is the equilibrium temperature for a natural water body. If heat rejection occurs, the surface temperature rises till the surface energy loss equals the heat rejected. The slope of the curve, at the equilibrium temperature, gives the overall heat transfer coefficient. A frequently employed expression for the surface energy exchange is:

$$H = h(T_s - T_e), \qquad (2\text{-}5)$$

where H is the surface energy loss per unit area, h the heat transfer coefficient, T_s the surface temperature, and T_e the equilibrium temperature, determined from curves similar to those in Fig. 2-5. For Cayuga Lake in New York State, h is 16.56 W/m^2-K during the winter and 24.61 W/m^2-K during the summer, with T_e in °C given by:

$$T_e = 10.67 - 16.28 \cos \left[\frac{2\pi}{365}(\tau - 19)\right] , \qquad (2\text{-}6)$$

where τ is time in days from January 1 (Moore and Jaluria 1972). For a solar pond, the various energy transfer mechanisms may be studied numerically and h

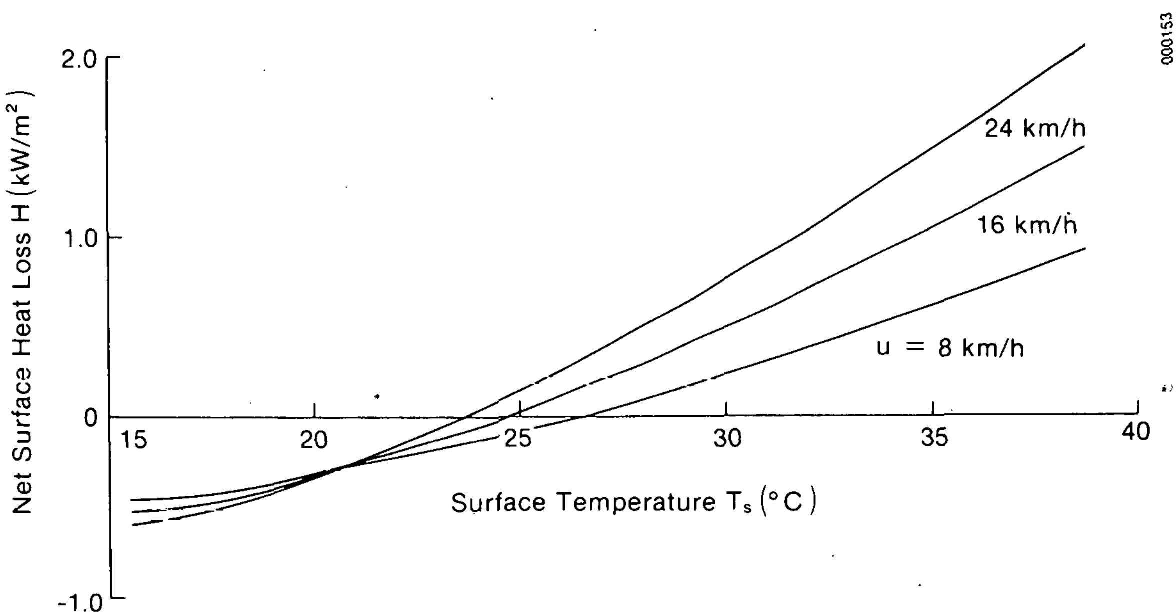

SOURCE: Jaluria 1979

Figure 2-5. Heat Loss at the Surface of a Water Body as a Function of the Surface Temperature for Various Values of Wind Speed

and T_e determined. Both h and T_e may be computed at various times during the year without curve fitting as done for Cayuga Lake. Results presented earlier indicate that h varies from about 15 W/m^2-K to 25 W/m^2-K and a suitably computed value may be used.

If the heat rejected to the solar pond per unit area is given, the average surface temperature rise and the increase in evaporation may be determined by using the treatment previously outlined. For a 34.5-W/m^2 heat rejection and h computed as 20 W/m^2-K, the average surface temperature increase would be 1.7°C, which is the typical temperature rise expected by heat rejection from a 3-MW power plant to a 1-km^2 solar pond. The equilibrium temperature is 27°C with heat rejection. Without heat rejection, it is about 27 - 1.7 = 25.3°C. If evaporation is calculated, the rise in temperature increases natural evaporation approximately 15%. This increase is about 1% of the flow rate for heat rejection with a temperature of 10°C between inflow and outflow. Therefore, the surface energy exchange may be computed to determine the surface temperature increase and the increase in evaporation caused by heat rejection.

The previous discussion was based on a steady-state analysis. However, the problem is time dependent since the ambient conditions vary during the day and over the year. Therefore, a study of the transient behavior is important in evaluating the performance of the solar pond. A quasisteady approach may be adopted with the variation in the ambient conditions taken as constant but using different values over specified periods of time. This will yield information on the behavior at various times during the year. For the variation from day to night, the transient terms must be included

(Foster 1971). If the surface layer is taken as isothermal, an energy balance gives:

$$\rho C_p V \frac{dT}{d\tau} = -HA \qquad (2\text{-}7)$$

where V is the volume of the layer, A the surface area, ρ the fluid density, C_p the specific heat, and H the net surface energy loss per unit area. This gives the temperature variation with time. Generally, a significant temperature variation exists across the surface layer, and a two-dimensional, vertical, transient model is more appropriate.

2.3 INTERFACE STABILITY

The effect of the heat rejection flow on the interface with the gradient zone must be considered since a disturbance to the interface may increase the depth of the surface layer. Thickening of the surface layer reduces the energy reaching the storage layer, and each centimeter increase in depth reduces the operating temperature ~0.5°C. The gradient layer is nonconvective, since the density increases with depth because of the salt distribution, despite the destabilizing effect of the temperature distribution. However, when heat rejection sets up a flow field, the flow has a destabilizing effect and tends to overturn the stably stratified region. If the velocity is high enough, it will overturn the gradient region to some depth, increasing the depth of the surface layer.

A comparison between the stabilizing density gradient and the destabilizing effect of the shear flow may be made using the local Richardson number Ri as considered by Lofquist (1960), Miles (1961), Turner (1965, 1973), Moore and Long (1971), and Crapper and Linden (1974), where:

$$Ri = \frac{g}{\rho}\frac{\partial \rho}{\partial z} \Big/ \left(\frac{\partial u}{\partial z}\right)^2 , \qquad (2\text{-}8)$$

where g is the acceleration caused by gravity, z the vertical coordinate, and u the shearing velocity as shown in Fig. 2-6. The problem may be considered in terms of the density and velocity gradients at the interface or the finite density and velocity differences across the layer, as seen in Fig. 2-6. According to the detailed study of Miles (1961) and discussed by Turner (1973), the stratification is stable against the shear flow if $Ri \geq 1/4$. This result, which is derived from various simplifying assumptions, has been used extensively for studying the stability of stratified media. The critical value of Ri varies somewhat for different flows [see Moore and Jaluria (1972) who employed this criterion for natural lakes].

If we consider a heat rejection H of 34.5 W/m^2 to the surface layer and a temperature difference ΔT of 10°C between the inflow and the outflow, the flow rate Q for a 1-km^2 pond is:

$$Q = HA/\rho C_p \Delta T. \qquad (2\text{-}9)$$

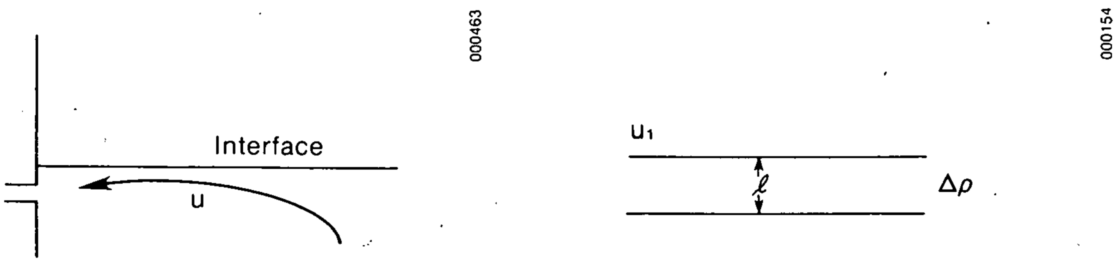

(a) $$Ri = \frac{g}{\rho}\frac{\partial \rho}{\partial z} \Big/ \left(\frac{\partial u}{\partial z}\right)^2$$

$\geq 1/4$, for stability

(b) $$Ri = \frac{g}{\rho}\frac{\Delta\rho}{(u_1 - u_2)}\,\ell = \frac{g\,\Delta\rho}{\rho\,\Delta u}\,\ell$$

$\geq 1/4$, for stability

Figure 2-6. Interface Stability

This gives the flow rate as 0.89 m^3/s. If a two-dimensional flow is considered with a slot width of 3 cm, the velocity at the inflow for a 1-km × 1-km pond is 0.03 m/s. If a linear velocity drop to the interface is taken to evaluate $\partial u/\partial z$, Ri is estimated at 87.1 for a 20-cm-deep surface layer. This value, which is obtained using a linear density variation across the gradient layer of ~20% by weight over 1 m, indicates that the stratification is very stable, and the flow is unable to overturn it. For Ri $\geq$ 0.85, there is no entrainment from the stratified region, which indicates the condition for negligible disturbance to the interface and requires that the flow channel centerline be at least 3 cm from the interface. If the inflow and outflow are located at the surface, which is ~20 cm from the interface, disturbance to the gradient zone will be even smaller. If the total gradient zone is considered, as shown in Fig. 2-6b, the zone again appears to be extremely stable to the shear flow.

The slot width and distance from the interface may be chosen on the basis of stability. In general, the density gradient at the interface will be larger than that approximated by the linear variation (see Fig. 2-1). The velocity distribution also is not linear, and a polynomial variation may be considered for greater accuracy. Note that the velocity gradient at the interface, calculated as a linear variation from the maximum velocity at the inlet, is overestimated, since the flow spreads out in the surface zone resulting in much lower velocities. Therefore, the earlier estimates of Ri are conservative.

2.4 TEMPERATURE DECAY AND RECIRCULATION

The circulating flow was sketched qualitatively in Fig. 2-2. A simple model for studying the horizontal decay of temperature away from the inflow assumes an isothermal surface layer. This is probably a fairly accurate model since wind and surface waves do lead to convective mixing in this layer. For a two-dimensional flow this assumption makes the problem one-dimensional and is governed by the equation:

$$u \frac{dT}{dx} = \varepsilon_H \frac{d^2T}{dx^2} - \frac{H(x)}{\rho C_p D} , \qquad (2\text{-}10)$$

where u is the averaged flow velocity in the direction of discharge x, ε_H is the thermal diffusivity, H the energy loss per unit area, and D the depth of the layer. The surface energy loss H obviously depends on the ambient conditions and the surface temperature. Figure 2-7 shows the typical temperature decay away from the inflow for a pond 100 m long. The equilibrium temperature is 25°C. At low heat-rejection rates, the outflow temperature remains unchanged. For large values of heat rejection the outflow temperature increases causing a corresponding increase in the inflow temperature for a given temperature difference ΔT. This figure indicates the amount of heat that may be rejected without significantly raising the outflow temperature. Similarly, we can determine the minimum distance between inflow and outflow that does not alter the outflow temperature if the heat rejected per unit area is low enough to allow the heat input to be lost in a distance less than the pond length. For a 34.5-/m² heat rejection to a 1-km × 1-km solar pond, we found that if the conduction term in Eq. 2-10 is neglected, the outflow should be 400 m or more away from the inflow. A computer can solve the equation including the diffusion term for more precise results. The eddy diffusivity may be estimated from earlier studies; e.g., from the works of Sehgal and Jaluria (1979), Wada (1967a,b; 1968a,b) and Foster (1971).

Several investigators have studied the recirculating flow in enclosures caused by the discharge of hot, buoyant fluid particularly for laminar flow. Wada (1967, 1968), Park and Schmidt (1973), Oberkampf and Crow (1976), Cabelli (1977), Sliwinski (1980), Gupta and Jaluria (1980, 1981), and Jaluria and Gupta (1980) studied the recirculating flow in water bodies for various flow configurations. Figures 2-8 through 2-10 indicate some of the results. Buoyancy drives the flow upwards causing it to stay close to the surface, resulting in a sharp temperature drop away from the surface. This results in a thermally-stratified surface layer with a small temperature increase at the interface, indicating a small disturbance to the gradient zone. Figure 2-10 shows the nature of the temperature profiles that may be expected. However, these results are for the transient case. The steady-state results should be similar since the input of energy is lost to the environment as the flow moves away from the inflow. Mixing in the layer caused by winds and surface waves tends to reduce this stable thermal stratification. But in regions close to the inflow, up to about 100 m (obtained from the Richardson number criterion), the thermal discharge provides stability against the mixing or convective effects. Therefore, the temperature profiles would be of the form seen in Fig. 2-10 near the inflow and fully mixed, or isothermal away from it. The discharged flow is quite similar to a buoyant surface jet. This consideration

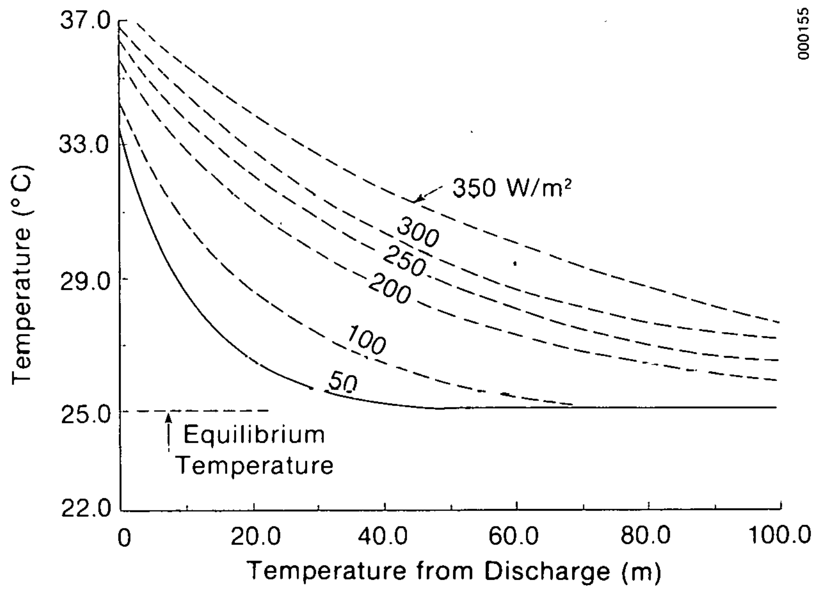

SOURCE: Sehgal and Jaluria 1979

Figure 2-7. Temperature Distribution in One-Dimensional Horizontal Flow with Heat Loss at the Surface for Different Heat-Rejection Rates ($\varepsilon_H = 10^{-5}\ m^2/s$).

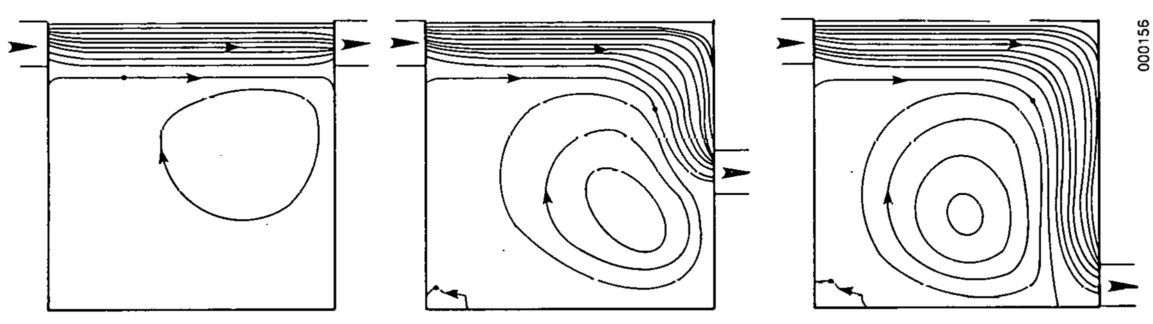

SOURCE: Oberkampf and Crow 1976

Figure 2-8. Streamlines for Outflow at Various Depths ($\Delta\psi = 0.01$, Re = 1.300)

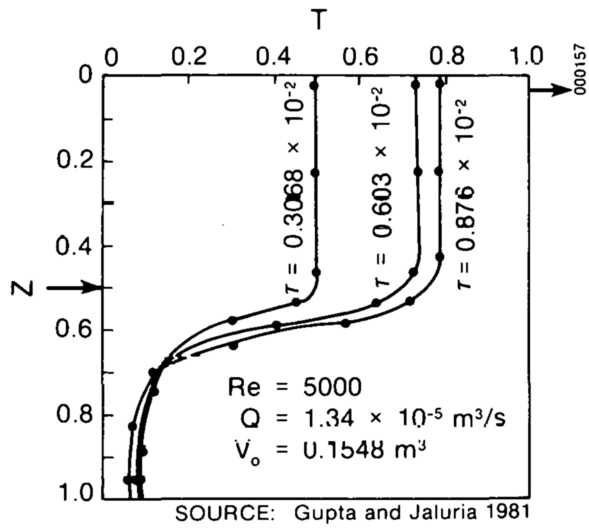

Figure 2-9. Transient Nondimensional Temperature Profiles in an Enclosed Water Body. The arrows indicate directions of inflow and outflow.

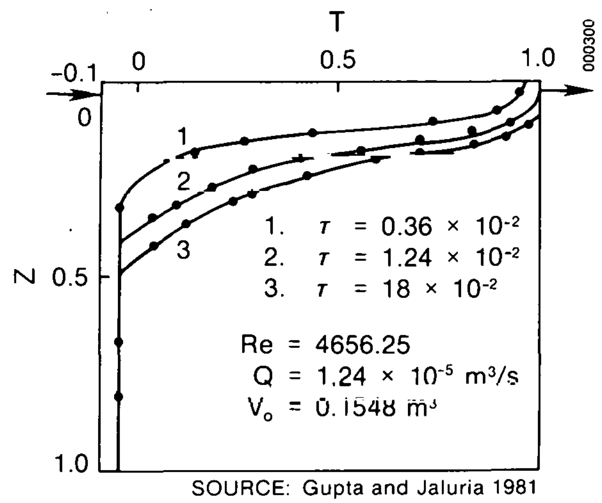

Figure 2-10. Temperature Profiles in an Enclosed Water Body with Inflow and Outflow Located at the Top on Opposite Sides

is discussed in Sec. 3.2 in terms of the penetration of flow in energy extraction from the storage zone.

2.5 GOVERNING PARAMETERS AND FUTURE WORK

The physical variables in the heat rejection problem are the ambient conditions, location of inflow and outflow channels, and:

- total heat rejected H_r,
- surface area of the pond A,
- flow rate Q,
- ambient conditions P_a,
- height of flow channels h_o,
- location of inflow and outflow channels Z,
- depth and length of the surface layer D, L, and
- density gradient at the interface with the gradient zone $\partial\rho/\partial z$.

The governing equations are the continuity, momentum, and energy equations for a two-dimensional flow. A buoyancy term appears in the momentum equation. With the Boussinesq approximations, the equations (Jaluria 1980) may be written as:

$$\frac{\partial u}{\partial x} + \frac{\partial v}{\partial y} = 0 \quad \text{(2-11a)}$$

$$\frac{\partial u}{\partial \tau} + u\frac{\partial u}{\partial x} + v\frac{\partial u}{\partial y} = -\frac{1}{\rho}\frac{\partial p}{\partial x} + \nu\left(\frac{\partial^2 u}{\partial x^2} + \frac{\partial^2 u}{\partial y^2}\right) \quad \text{(2-11b)}$$

$$\frac{\partial v}{\partial \tau} + u\frac{\partial v}{\partial x} + v\frac{\partial v}{\partial y} = -\frac{1}{\rho}\frac{\partial \rho}{\partial y} + \nu\left(\frac{\partial^2 v}{\partial x^2} + \frac{\partial^2 v}{\partial y^2}\right) + g\beta(T - {}_aT\ ) \quad \text{(2-11c)}$$

$$\frac{\partial T}{\partial \tau} + u\frac{\partial T}{\partial x} + v\frac{\partial T}{\partial y} = \alpha\left(\frac{\partial^2 T}{\partial x^2} + \frac{\partial^2 T}{\partial y^2}\right) \quad \text{(2-11d)}$$

where

u,v = velocity components in the horizontal x and the vertical y directions, respectively;

τ = time;

p = pressure;

ν = kinematic viscosity;

α = thermal diffusivity; and

β = coefficient of volumetric thermal expansion.

For turbulent flows, both ν and α are replaced by the corresponding sum of molecular and eddy components (Jaluria 1980). The boundary conditions are the no-slip conditions on the walls, slip conditions on the upper and lower boundaries with no normal penetrative flow, adiabatic conditions on the walls (or an energy transfer, if known), surface energy exchange at the top surface, and conduction gain at the interface with the gradient layer. The top and bottom surfaces may be taken as known streamlines. This is obviously a fairly complicated problem and could be solved by finite-difference methods on a computer. However, we shall consider the basic features of the problem here and discuss the governing parameters.

If Eqs. 2-11a,b,c,d are nondimensioned with the characteristic inlet velocity and the height of the inflow channel, the three dimensionless parameters that arise are:

$u_o h_o/\nu$ = Reynolds number (Re);

$U_o/(g\beta h_o \Delta T)^{1/2}$ = Froude number (Fr); and

D/L = aspect ratio.

In addition, the Richardson number Ri defined in Eq. 2-8 becomes an important parameter that characterizes the stability of the interface and determines if the assumption of no flow normal to the interface is valid. Note that Ri may be described as $Ri = 1/Fr^2$, if a linear variation across the layer of height h is taken for ρ and u. However, the two are kept distinct because Fr is considered at the entrance and Ri in regions far from the inlet. For a laboratory study, these parameters must be simulated. However, a condition of $Ri \gtrsim 1.0$ would be adequate for modeling a stable interface in the laboratory, even if Ri is much larger in actual pond conditions. Similarly, in turbulent flow the Reynolds number only has to be large enough to give rise to a fully turbulent flow. The results would probably be quite sensitive to all three parameters, Re, Fr, and D/L, and it would be desirable to simulate them in the laboratory as closely as possible. However, if an analytical study is done concurrently with the experiments, the analytical model initially may be used to predict observations in the laboratory and then used, with modifications, to predict actual conditions in a pond.

Also note that it is difficult to simulate energy exchange mechanisms at the surface because of different ambient conditions, surface waves, and wind effects. The heat transfer coefficient may be approximated by providing a fan or a blower, but differences would remain and an analytical study would be desirable. In the laboratory, the resulting thermal and flow fields could be studied, providing information on the effect of the flow on the interface and on the various other aspects discussed earlier. The transient aspects could best be studied in the laboratory; but analytical work is required to answer several important questions raised in the earlier discussion. Table 2-1 summarizes the important conclusions obtained in this preliminary study.

Table 2-1. Summary of Results for Heat Rejection

(3-MW plant on 1-km^2 pond with thermal to electric efficiency η_T = 8%)

1. Average surface temperature rise is about 2°C.
2. Increase in evaporation is about 1% of flow rate.
3. Surface energy loss is mainly due to evaporation and back radiation.
4. Interface is stable.
5. Outflow must be more than 400 m from inflow.
6. If $Fr \lesssim 1.0$, there is no entrainment.
7. Flow establishes in a few hours.
8. Inflow/outflow must be near surface.
9. Basic parameters are Re, Fr, D/L, Ri.
10. Further analysis on periodic behavior is needed.

SECTION 3.0

ENERGY EXTRACTION FROM THE STORAGE ZONE

3.1 THE PROBLEM

Energy may be extracted from the storage zone of a solar pond by using a recirculating fluid flow or by placing a heat exchanger in the storage layer. Nielsen (1976) uses the latter method, which relies on natural convection and requires a heat exchanger with a large surface area. In addition, immersing the heat exchanger into the pond causes cleaning and maintenance problems.

This section addresses the method of recirculating storage brine through an external heat exchanger. Two flow configurations are shown in Fig. 3-1. The top-to-bottom configuration is more desirable because it reduces piping costs, particularly for large ponds, and also reduces energy loss in the pipes. However, one must determine how far this flow penetrates into the storage zone before it recirculates to the outflow port. Since the flow must pass over the entire storage layer to extract energy, one must determine the maximum size of pond for which this configuration remains efficient. In the end-to-end configuration, the flow recirculates over most of the storage layer and, therefore, is suitable for energy extraction. The following sections describe the basic features of the two flow configurations and give preliminary information on the effect these will have on solar pond performance and energy extraction.

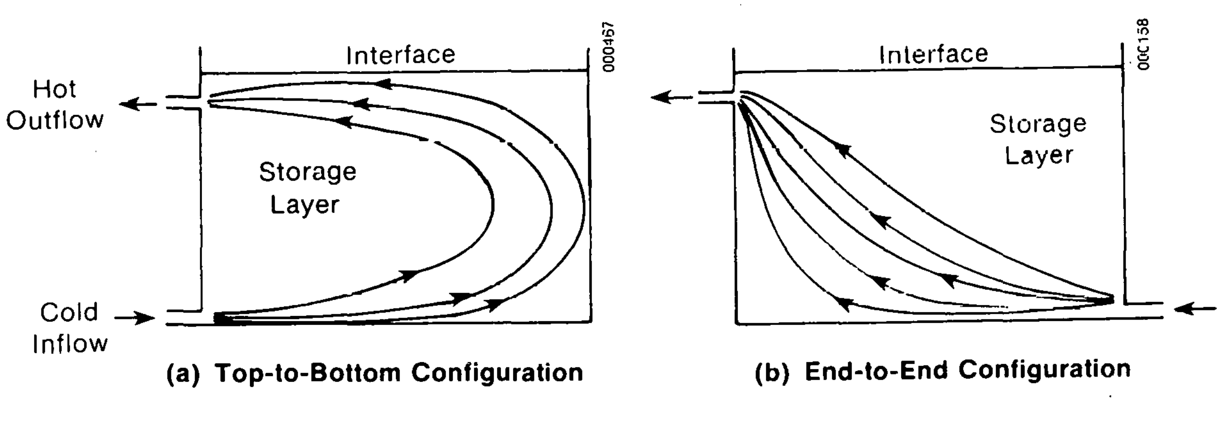

Figure 3-1. Flow Configurations for Energy Extraction

3.2 PENETRATION OF FLOW INTO THE STORAGE LAYER

For the top-to-bottom flow configuration, it is important to determine the distance in the storage layer that the recirculating flow penetrates. It involves analyzing the coupled temperature and flow fields governed by Eqs. 2-11a,b,c,d. The salt concentration is essentially uniform in the storage zone, so the problem may be treated using the thermal effects alone. However, the fluid is more dense in the storage layer than in the surface layer. Solving the governing partial differential equations is fairly complicated; therefore, it is desirable to estimate the penetration, which may be obtained from earlier studies on various idealized circumstances. Since no one has studied the recirculating flow in the storage zone in any detail, we will use the results of work done on heat rejection with modifications.

Among the most relevant studies of thermal discharge to water bodies are those concerning the surface buoyant jet, which has been considered by Jen, Weigel, and Mobarek (1966), Tamai, Wiegel, and Tornberg (1969), Koh (1971), Stolzenbach and Harleman (1973), Engelund (1976), Wiuff (1978), and McGuirk and Rodi (1979). This flow is very different from the nonbuoyant jet considered by Morton (1959), Abraham (1965), and List and Imberger (1973). The main difference is in the entrainment and consequent spread of the flow. Figure 3-2 shows a sketch of a two-dimensional, surface buoyant jet. As the fluid enters the water body, it entrains fluid, and the velocity and the temperature in the flow decrease. At a distance x from the source, the local Richardson number is defined as:

$$Ri = g \frac{\Delta\rho}{\rho} \frac{d}{U^2} \qquad (3\text{-}1)$$

where $\Delta\rho$ is the density difference from the ambient water medium, d the thickness of the flow region, and U the mean velocity in the flow. Ri may be defined as $1/Fr^2$. The entrainment into the flow depends on Ri.

Some studies have shown an interesting result concerning flow in stratified media. If the local Richardson number is greater than ~0.85, or the local Froude number is less than ~1.08, the entrainment of ambient fluid into the flow is negligible [see Ellison and Turner (1959), Wada (1967a,b; 1968a,b), Koh (1971), and Turner (1973)]. Therefore, as the flow slows down because of entrainment, the jet ceases to entrain, and a two-layered, stratified flow is set up. Beyond this point, shear forces and heat loss from the buoyant flow determine flow behavior. If good mixing is desired, Fr at the inlet should be kept large, and if a large penetration with negligible mixing is desired, $Fr \lesssim 1.0$. Figure 3-3 shows the spread of a two-dimensional jet and the decrease in temperature away from the inlet. The flow attains an almost constant thickness away from the inlet. These curves represent negligible heat loss; however, they do continue the interesting trend shown in Fig. 3-2. For very low Fr, the source is inundated, and the flow is simply a two-layered, stratified flow. Figure 3-4 shows the dependence of the velocity, temperature, and jet thickness on the entrance Richardson number Ri_o. We observed trends similar to those of Fig. 3-3 with the spread decreasing as Ri_o increases. These results indicate the tremendous importance of the entrance Froude number on the flow pattern downstream. Figure 3-5 also shows the effect of Fr on the entrainment and the resulting flow rate downstream.

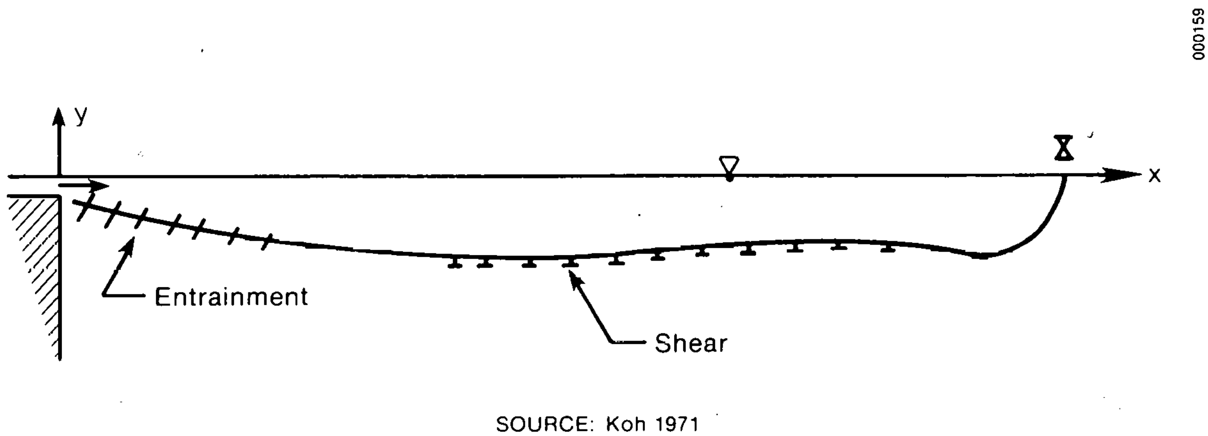

Figure 3-2. Two-Dimensional Surface Source of Buoyant Fluid

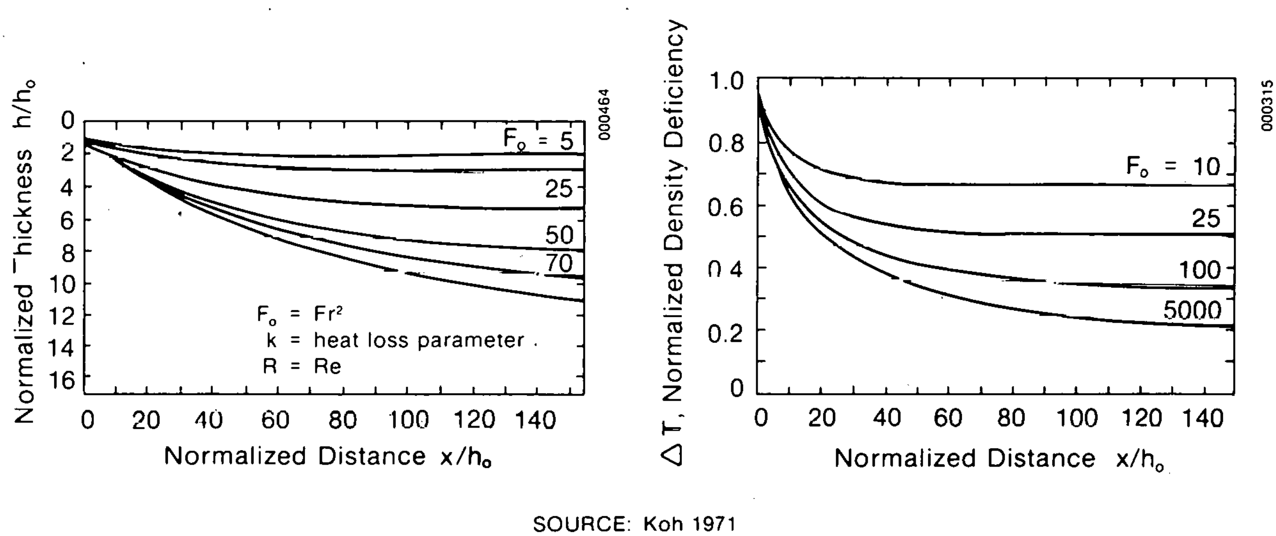

Figure 3-3. Predicted Jet Thickness and Density Deficiency in Surface Horizontal Buoyant Jet for $k = 1/R = 0$ (Two-Dimensional Case)

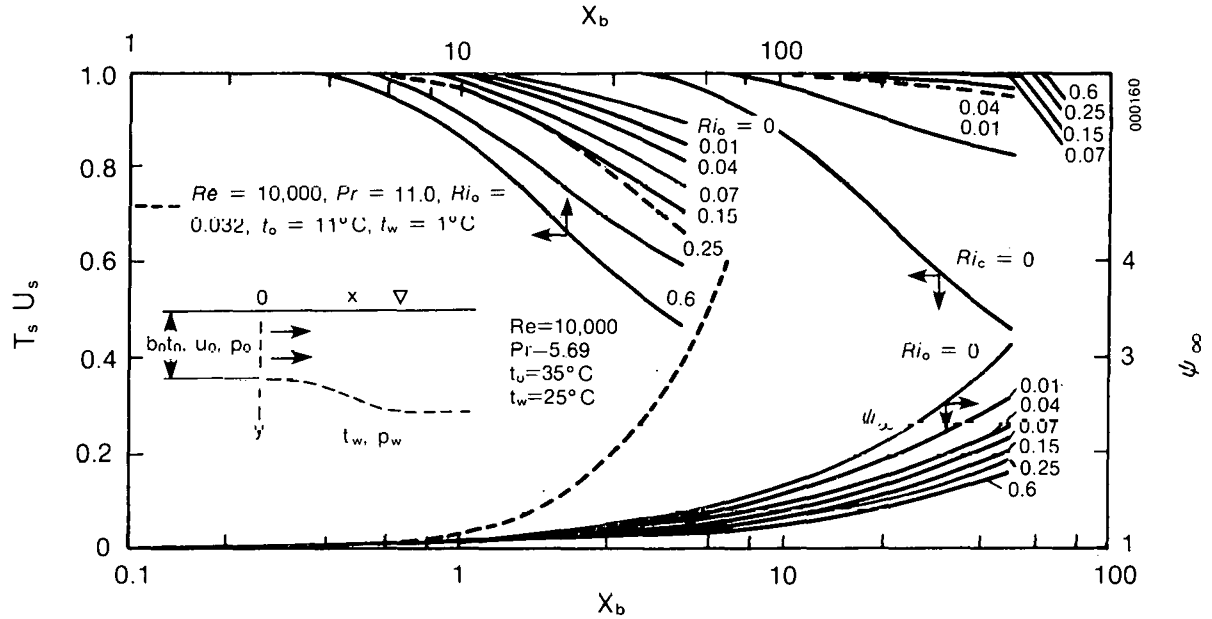

(a) Surface velocity, surface temperature, and flow rate

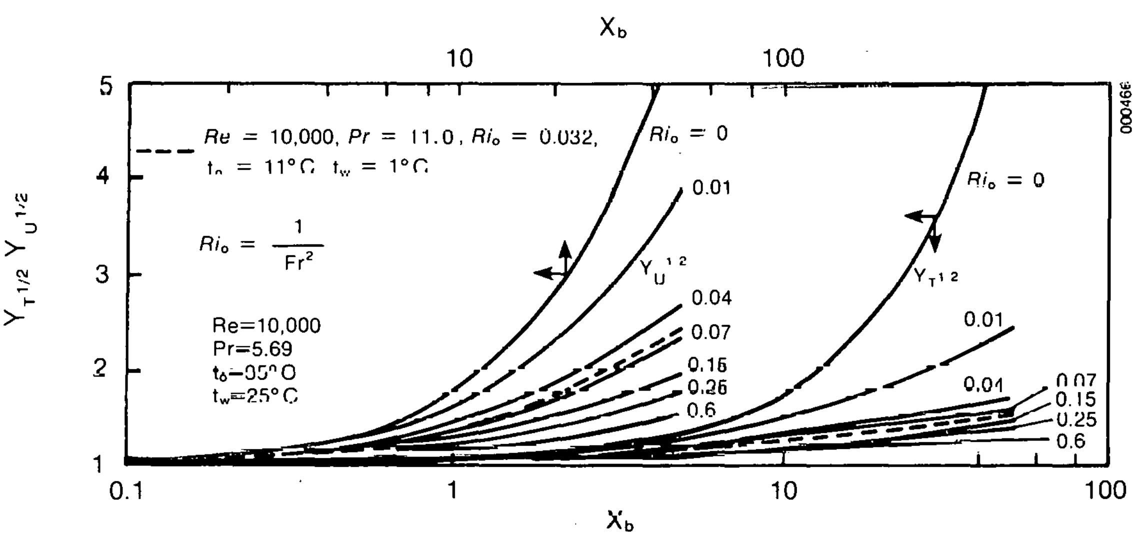

(b) Half-widths for velocity and temperature distributions

SOURCE: Miyazaki 1974

Figure 3-4. Dependence of Velocity, Jet Thickness, and Temperature on Entrance Richardson Number ($Ri_o = 1/Fr^2$)

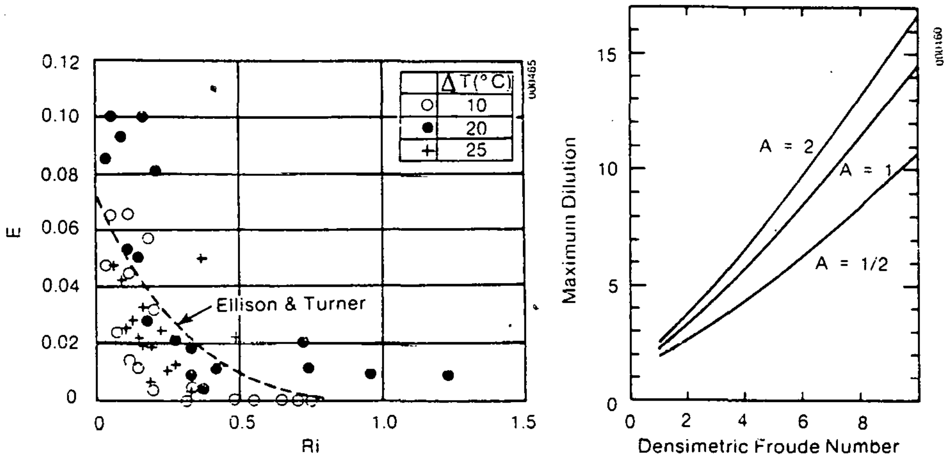

SOURCE: Wada 1969

(a) Entrainment E as a function of Richardson number Ri

SOURCE: Stolzenbach and Harleman 1973

(b) Calculated dilution in the stable region vs. the initial densimetric Fr and the discharge channel aspect ratio $A = h_o/b_o$

Figure 3-5. Dependence of Entrainment and Downstream Flowrate on the Froude Number Fr ($Fr^2 = 1/Ri$)

If a slot width of 1 cm is considered for a flow of 10^{-3} m^3/s-m, Fr equals 4.4. This and all other calculations given in this report use the fluid property data obtained from the Saline Water Conversion Engineering Data Book (Office of Saline Water 1971) and Kaufman (1960). Therefore, with a slot width of 1 cm the jet behaves as shown in Fig. 3-2. However, if a slot width of 3 cm is taken, Fr equals 0.845, which corresponds to an entrance Ri of 1.4, leading to negligible entrainment and greater penetration of the flow. Two-layer stratification is expected in this case with energy exchange and shear at the flow boundaries determining the flow pattern. As long as the local Ri is greater than 0.85, there should be no entrainment. Shear reduces the velocity and, thus, increases the flow thickness, leading to a larger value of Ri, whereas energy loss to the environment reduces the density difference and tends to decrease Ri. Therefore, it is important to determine the rate of temperature and velocity decrease and the increase in flow thickness. Since $Ri \propto \Delta T$, where ΔT is the temperature difference between the flow and the ambient, ΔT must decrease by about 40% in the absence of shear for Ri to decrease from 1.4 to 0.85. In practice, of course, shear tends to increase Ri, and the distance needed for Ri to attain a value of 0.85 is much larger. Researchers have also considered thermal discharge into stratified media, and Fig. 3-6 shows the nature of penetration as obtained by Darden, Imberger, and Fischer (1975).

Heat extraction involves a cold water inflow near the bottom of the tank and a hot water outflow from a port located below the interface with the gradient zone, as shown in Fig. 3-1. Therefore, the inflow of cold water is similar to the buoyant surface jet flow except for a solid boundary being present at the bottom and, consequently, a larger surface shear effect. The inflowing water is heavier than the ambient hot water in the storage layer. Because of energy

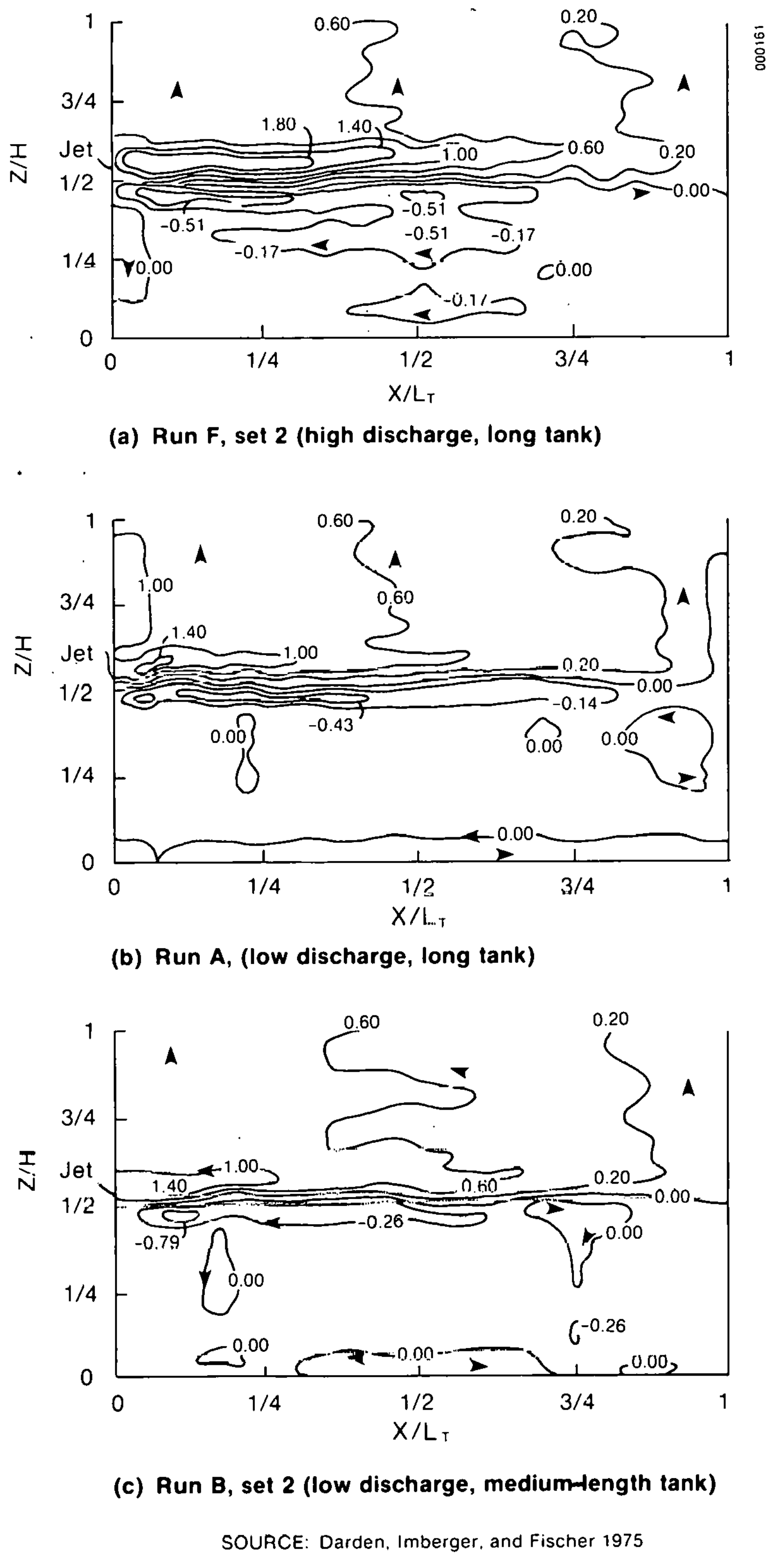

Figure 3-6. Streamline Plot Ψ/Q

gained from the solar flux absorbed at the bottom and of conduction from above, the inflowing water heats up as it moves away from the inlet.

Let us consider a two-dimensional flow with a flow rate Q of m^3/s-m and a temperature defect from the ambient hot fluid in the storage layer of $(\Delta T)_o$ at the entrance. If Fr $\lesssim$ 1.0, the entrainment from above is negligible, and a constant flow rate is maintained. If the flow gains q W/m^2, caused by heating from below and the energy transfer from above, the temperature difference ΔT at a distance x from the inlet is given by:

$$\Delta T = (\Delta T)_o - \frac{qx}{\rho C_p Q} \quad . \tag{3-2}$$

This equation is valid as long as there is no entrainment. Conduction in the flow direction is also neglected. The energy gain from below is about 20% of the incident solar flux at the surface. This gives a value of 40 W/m^2. The estimate of energy transfer from above caused by the existing stable stratification is more involved. The flow thickness varies from the slot width to a depth of approximately half the height of the storage layer. The temperature defect also varies from a typical inlet value of 10°C to a much smaller value at which entrainment and continuity make the flow turn back towards the outflow channel. The source would be inundated if Fr $\lesssim$ 1.0; therefore, determining the energy transfer to the flow from above requires further information on flow spread, temperature, and velocity decay. In the absence of this information, the transfer of heat from above may be estimated near the source by considering a temperature field spread of ~5 cm (for a slot width of 3 cm) and far from the source by assuming the spread to be half the height of the storage zone. The former gives a heat flux of about 120 W/m^2, and the latter about 1 W/m^2. One may thus take an average of 60 W/m^2 added to the gain of 40 W/m^2 from below. Then, with a total heat input into the flow of 100 W/m^2, a distance of 400 m is needed (from Eq. 3-2) to lose the entire buoyancy effect.

The estimated distance over which the flow loses its buoyancy defect might be improved by considering the temperature-dependent heat conduction from above. An exponential temperature decay arises in that case and, again, about 400 m are needed for the buoyancy defect to be negligible. This is the maximum penetration to be expected. Shear and pressure, which are caused by the basic conservation principles as embodied in Eqs. 2-11a,b,c,d, will reduce it.

The shear effect on the flow may again be estimated by using a simple model based on the no-entrainment situation for Fr $\lesssim$ 1.0. Let us consider a slot width of 3 cm and a flow rate of 10^{-3} m^2/s, which implies a total flow of 1 m^3/s over a 1-km-wide pond. The inlet velocity is 3.3×10^{-2} m/s, the coefficient of viscosity μ is 6.3×10^{-4} kg/m-s, and the shear stress at the bottom is $\mu\, \partial u/\partial y$, where y is the vertical coordinate. Since there is no entrainment, the flow rate is constant at 10^{-3} m^2/s. For example, let us calculate the distance L needed for the velocity to drop to one-third the value at the inlet. At this velocity level, the spread of the flow must be 9 cm to conserve the flow rate. Estimating the velocity gradient is difficult because we do not know the actual velocity profiles in the flow. However, it may be estimated as U/d, where U is the average velocity level over a given distance and d the average half-depth of the flow. For a two-layered flow, one expects an essentially linear profile, and this estimate should be reasonable.

The principle of momentum force balance says

(Mass flow rate) × (decrease in velocity) = (force acting on the fluid); (3-3)

therefore,

$$\left(1.0887 \times 10^{3} \times 10^{-3}\right) \times \left(\frac{2}{3} \times 3.3 \times 10^{-2}\right) = \left(6.3 \times 10^{-4} \times \frac{2.2 \times 10^{-2}}{3 \times 10^{-2}}\right) \times L$$

or L = 51.8 m.

One can easily show that the pressure effect is negligible compared to the shear torce. Similarly, one can show that the distance L for the velocity to drop to one-tenth the value at the inlet is 233 m. The estimate for the shear stress is probably higher than the actual value, since the source would be inundated and the depth of the flow in the region near the source would be larger than the slot width. The temperature defect at 233 m is about 4°C, as obtained from Eq. 3-2. The velocity level is 3.3×10^{-3} m/s and the spread of the flow is 30 cm. One can show that Ri > 0.85, and no entrainment occurs in the flow. Since a negligible buoyancy defect is expected beyond 400 m, Ri must drop below 0.85 before that, and entrainment will occur leading to a rapid mixing and recirculation of the flow to the outlet. One could calculate the velocity level and the flow spread up to 400 m. However, the presence of the outflow would cause recirculation, and, as the buoyancy effect and the velocity level decrease, the flow turns back after penetrating a certain distance into the storage layer. Some of these considerations are outlined in Sec. 3.3.

3.3 FLOW RECIRCULATION

The penetration of the flow into the storage layer largely was considered as a cold, stratified layer flowing under a warmer, lighter fluid in the storage region. Considering the flow as being stratified into two layers or as a surface jet assumes that no outflow exists that would affect the flow. However, in actuality, an outflow port is located at the other end of the pond for the end-to-end extraction or above the inlet on the same side for the top-to-bottom extraction. In both cases, the outflow affects the flow pattern considerably, and a recirculating flow arises, as shown in Figs. 3-7 and 3-8 for a heated discharge into an enclosed water body.

The recirculating flow, even if a heated discharge, has received very little attention in literature, despite its tremendous importance in designing such systems. Wada (1967a,b; 1968a,b), Oberkampf and Crow (1976), Gabelli (1977), Sehgal and Jaluria (1979), Jaluria and Gupta (1980), and Brocard and Harleman (1980) have done some work in this area. The work of Wada (1967a,b; 1968a,b) largely relates to heat rejection in oceans; the other studies pertain to the laminar flow under certain idealized conditions. Essentially no work has been

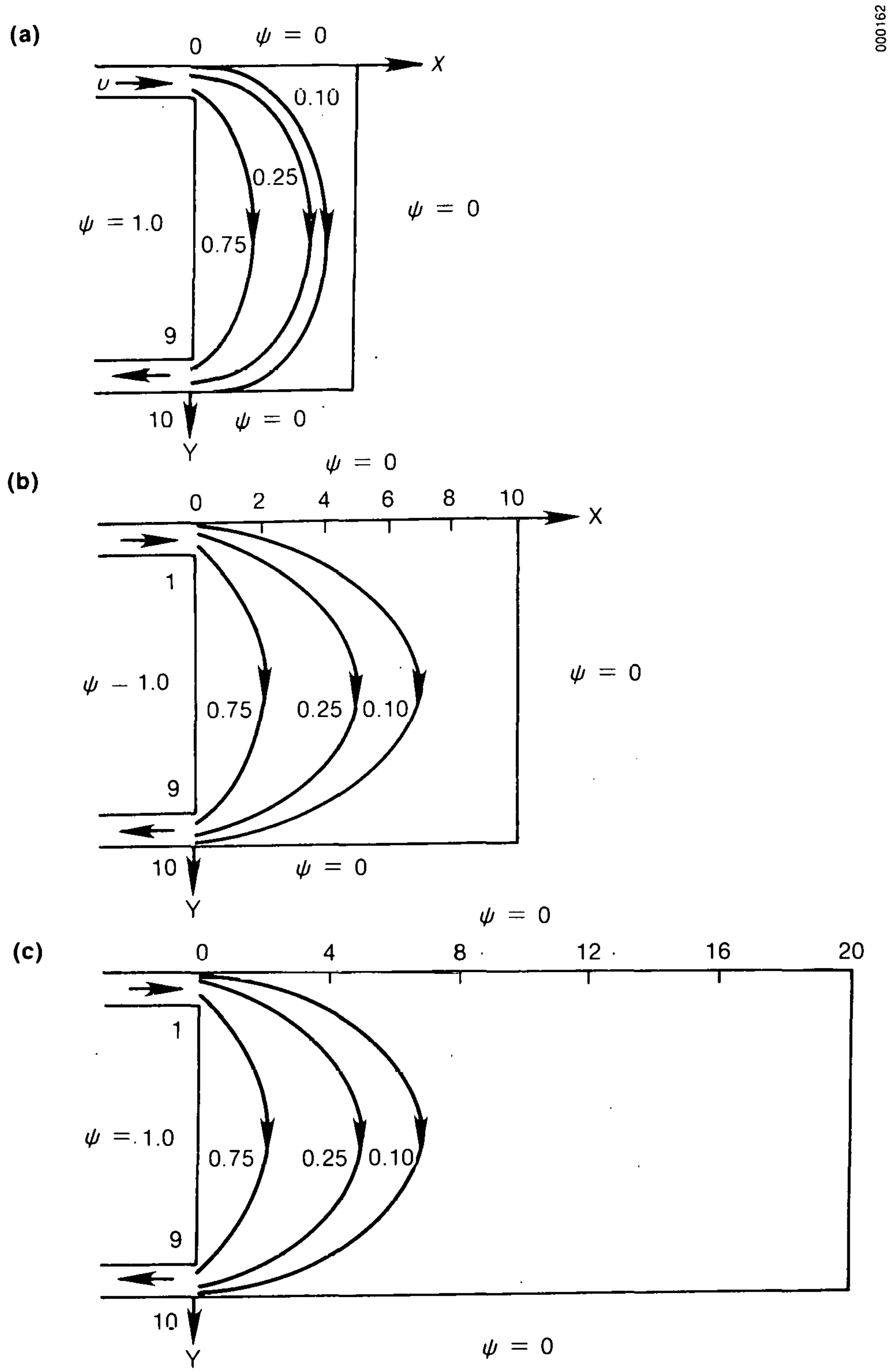

SOURCE: Sehgal and Jaluria 1979

Figure 3-7. Two-Dimensional Horizontal Flow with Intake and Outfall on the Same Side for Various Values of the Aspect Ratio D/L of the Water Body

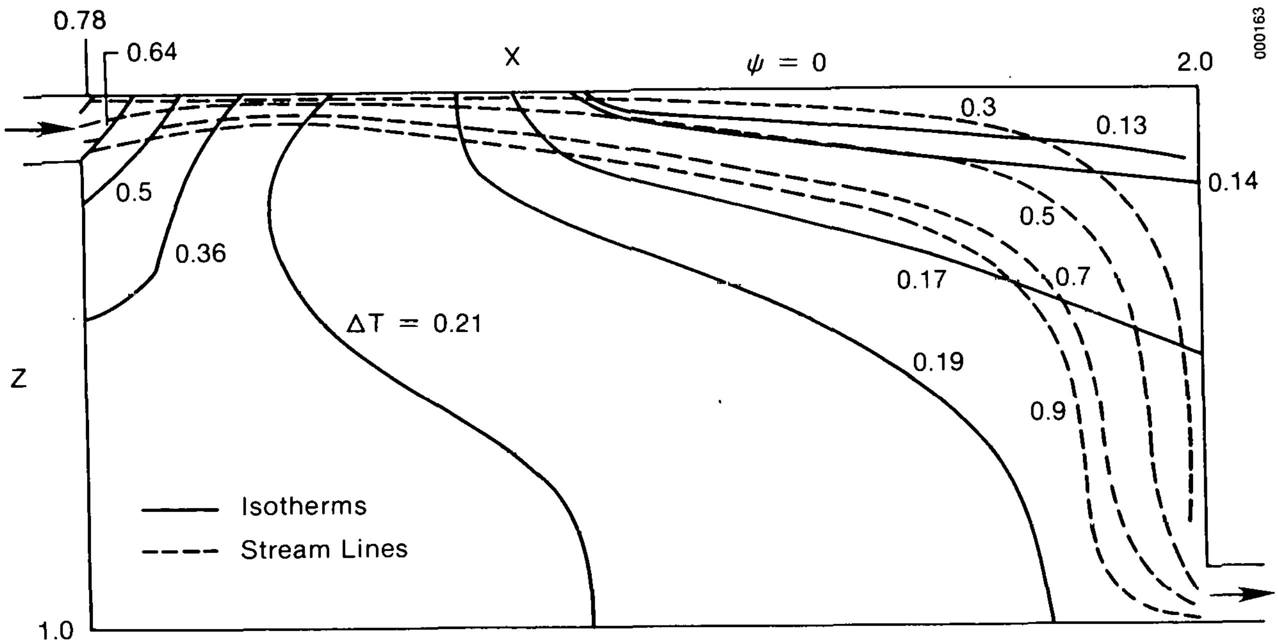

SOURCE: Jaluria and Gupta 1980

Figure 3-8. Steady-State Solution at Gr/Re^2 = 12.3, Re = 50 ($Fr = Re/Gr^{1/2}$)

done on the energy extraction problem. The work of Lavan and Thompson (1977), although related to energy extraction, uses a very small tank and does not consider the recirculating flow.

In the top-to-bottom configuration (shown in Fig. 3-7), the flow only penetrates a certain distance into the storage zone leaving the remaining portion essentially unused for energy extraction. It is necessary to determine this distance and to study energy extraction from the region in which the flow is negligible. Figure 3-9 shows this situation qualitatively. Solar flux is absorbed also in the region on the right where there is essentially no flow. This absorbed energy is to be extracted largely by natural convection, arising due to horizontal temperature gradients. The aspect ratio D/L of this region is very small, and the horizontal temperature differences lead to a weak natural convection flow [see Bejan and Tien (1978) and Bejan and Imberger (1979)]. The temperature profiles are expected to be as shown. The heat transfer coefficient for energy transfer from the right to the flow region on the left may be determined from the above references.

Bejan and Tien (1978) give the heat transfer correlation for a long horizontal cavity as:

$$q = h\Delta T = \frac{k}{L}\,\Delta T \quad 1 + \left(\left\{\left[\frac{(RaD/L)^2}{362880}\right]^n + (0.623\ Ra^{1/5}L/D)^n\right\}^{1/n}\right) \qquad (3\text{-}4)$$

where

q = heat transfer per unit area across the horizontal cavity,

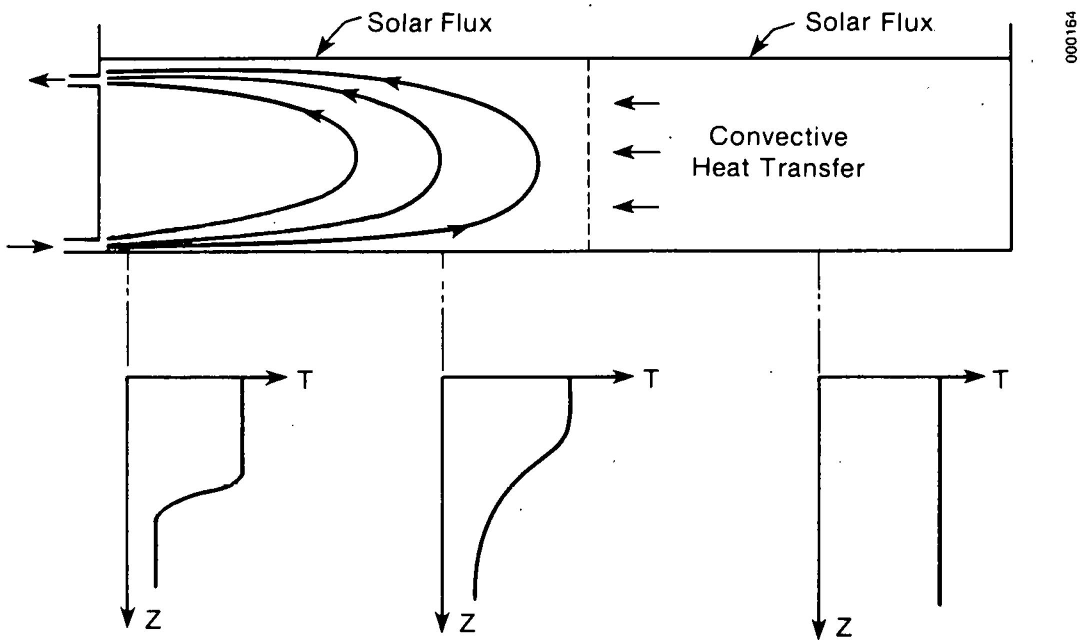

Figure 3-9. Energy Extraction from Region with Negligible Flow

ΔT = temperature difference,

k = fluid thermal conductivity,

Ra = Rayleigh number defined as

$$Ra = g\beta D^3 \Delta T/\alpha\nu, \text{ and} \quad (3\text{-}5)$$

n = -0.386.

The heat transfer coefficient h may be determined from this equation. Since the aspect ratio D/L is very small, the last term (in parentheses) dominates, giving the boundary layer regime for which the heat transfer coefficient is given by:

$$h = \frac{k}{D}\, 0.623\ Ra^{1/5} \quad (3\text{-}6)$$

Equation 3-6 gives h as 55 W/m^2 K for ΔT = 1°C and 87 W/m^2 K for 10°C. If a temperature difference of 10°C is allowed in the region on the right, we may determine the length of the region ℓ from which the absorbed solar energy is extracted. For a solar flux absorption in the storage layer of 40 W/m^2, the energy absorbed over a length ℓ is 40ℓ W/m. Equating this to the convective energy transfer to the flow region on the left gives

$$40\ell = 87 \times 10 \times D \quad .$$

For D = 1 m, this gives ℓ = 21.8 m. Therefore, the energy absorbed over 21.8 m of the region of the right is extracted by the recirculating flow due to natural convection, assuming a 10°C allowable temperature drop. This indicates that one might expect the thermal effects to penetrate ~25 m beyond the region of the recirculating flow because of natural effects arising from the horizontal gradients. Wind-induced mixing and surface waves tend to increase this distance.

In the top-to-bottom flow configuration, one has to consider the effect of an outflow channel on the cold fluid flowing into the storage zone. Yih (1958, 1960), Debler (1959), Kao (1963, 1965, 1976), Koh (1966), Wood (1968), Imberger (1972), Pao and Kao (1974), Imberger and Fandry (1975), Imberger, Thompson, and Fandry (1976) and Bryant and Wood (1976) considered various aspects of withdrawal from a stratified environment and determined conditions under which only the fluid at the same horizontal level as the outflow channel is withdrawn (selective withdrawal). Turner (1973) and Yih (1980) discuss the basic features of this problem on the basis of these various studies.

Of particular interest is the spreading of the flow away from the withdrawal port. For a two-dimensional flow, Koh (1966) showed that the thickness of the withdrawal layer δ varies as $x^{1/3}$ and the velocity level varies as $x^{-1/3}$. The variation of δ is given as:

$$\delta = 7.14x^{1/3}/\alpha_o \tag{3-7}$$

where

$$\alpha_o = (\varepsilon g/\alpha\nu)^{1/6} \text{ and } \varepsilon = -\frac{1}{\rho}\frac{\partial\rho}{\partial y} \tag{3-8}$$

(α is the thermal diffusivity). For the present problem, if the density difference is taken for a temperature difference of 10°C, it can be shown that δ = 35.7 cm at x = 100 m and about 45 cm at 200 m. At x = 1000 m, the spread of the flow is predicted to be 76.7 cm. Koh (1966) also compared his analytical results with experiments over the Re range of 0.3-100.4 and found good agreement. At larger Re, typical of ponds, the spread may be lower, as with boundary layer flows. Also, at the onset, withdrawal is from an unstratified medium, which gradually becomes stratified over time.

Earlier, the spread of the cold layer at the bottom was estimated to be 30 cm at 233 m. At this distance the withdrawal layer is estimated to be 47.3 cm. Therefore, for a storage layer 1 m deep, the two layers are expected to meet at a distance of about 350 m from the inlet. Recirculation occurs before the two layers meet because of the pressure field set up by considering continuity. The outflowing fluid pulls at the inflowing fluid, and continuity leads to the recirculation. Therefore, an estimate of the flow penetration into the storage layer may be taken as 300 m. For more accurate information on the penetration, the coupled flow and thermal fields must be solved numerically.

For the end-to-end extraction, the flow is as shown in Fig. 3-8. The cold, entering fluid stays near the bottom because of the buoyancy defect. Far from the inlet, when the buoyancy defect is small, the fluid rises to flow out of the tank. If the inflow is above the bottom, which is generally the case, the flow drops to the bottom because of the buoyancy defect, as studied by

Riester, Bajura, and Schwartz (1980) and shown in Fig. 3-10. The cold fluid then flows along the tank bottom towards the outlet. In this configuration, much of the fluid above the inflowing cold fluid is left untouched. Also, penetration of the flow into the storage layer is not a concern because a smaller penetration has less effect on the outflow temperature. Therefore, the entrance Froude number should be $\gtrsim 1.08$ so that the flow entering the storage layer mixes with the surrounding hot fluid and loses the buoyancy defect in a short distance. This is more important at night since there is no heat input because of the solar flux, and if good mixing is not ensured, the flow may convey the cold fluid to the outlet causing a temperature drop there. This condition of $Fr \gtrsim 1.08$ is contrary to that for the top-to-bottom configuration, where the buoyancy defect must be maintained to have a larger penetration. If good mixing of the entering fluid is ensured for the end-to-end configuration, a simple plug flow model may be used to determine the propagation of the thermal effects.

3.4 INTERFACE STABILITY

The stability of the interface between the storage and the gradient zones is very important in evaluating the effect of the flow on the nonconvective zone. A condition of $Ri \gtrsim 0.85$ ensures negligible entrainment into the flow from the stratified nonconvective zone. For a flow of 1 m^3/s over a width of 1 km, with a 3-cm slot width, one can easily show that the interface would be stable if the ports were located more than 3 cm from it. However, as seen in Fig. 2-1, the density gradient is much weaker at the interface between the storage and the nonconvective zones than between the surface and the nonconvective zones. Zangrando (1979) observed that the density gradient at the lower interface is about half the average gradient across the nonconvective zone. This implies that the ports should be located farther away from the interface. If the concentration gradient at the interface is taken as 10% by weight per meter, about half the average gradient in the nonconvective layer, a distance of 4 cm between the centerline of the outflow port and the interface gives $Ri = 1.07$. Since the density gradient at the interface may still be even weaker in certain cases, a distance of more than 6 cm may be necessary to stabilize the interface.

Since the velocity increases if the slot width is decreased, the separation between the flow channel and the interface would have to be larger to maintain the stability of the interface. A distance of 10 cm would be needed for a slot width of 1 cm for the same flow of 10^{-3} m^2/s. Previous discussions (Sec. 2.3) on interface stability indicate that flow diffusers must be designed and located suitably to have a negligible disturbance on the interface. Spreading out the inflow to obtain a two-dimensional flow pattern, increasing the slot width, and locating it as far as possible from the interface would not disturb the nonconvective zone. Discharging the same flow through a single pipe or locating the diffusers very near the interface would disturb the interface.

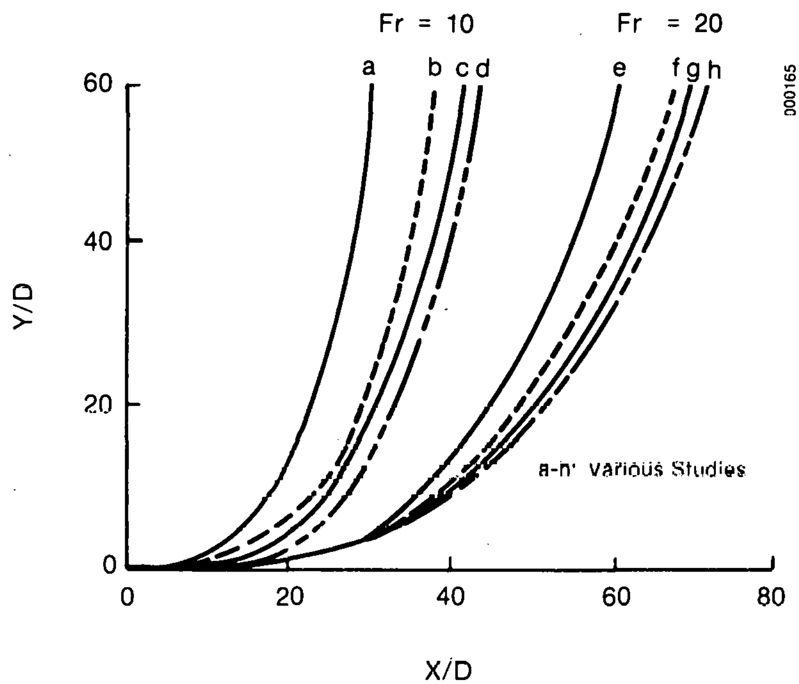

(a) Analytical predictions for the centerline trajectory of horizontal buoyant submerged jets for exit Froude numbers of 10 and 20

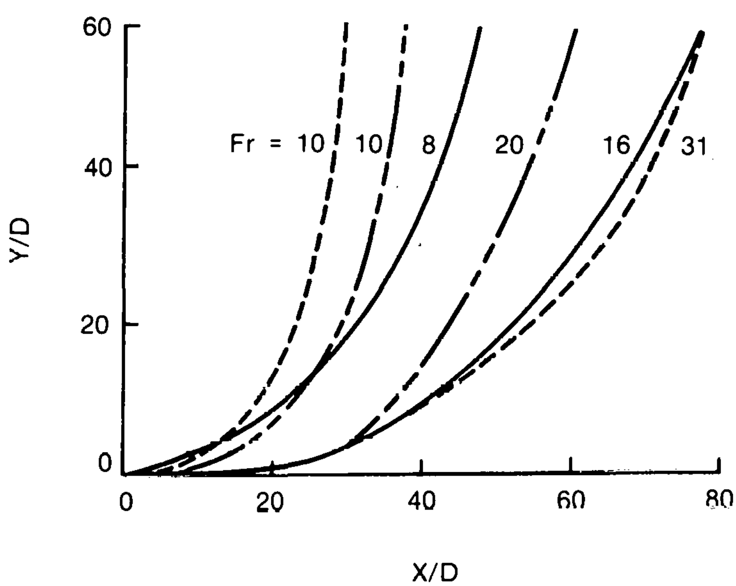

(b) Illustration of experimentally determined trajectories of horizontal buoyant submerged jets

SOURCE: Riester et al. 1980

Figure 3-10. Trajectories of Horizontal Buoyant Submerged Jets

3.5 GOVERNING PARAMETERS AND EXPERIMENTAL MODELING

Equations 2-11a,b,c,d describe the recirculating flow for a two-dimensional model. Since the inflow is at a lower temperature than the ambient water in the storage layer, the buoyancy term in Eq. 2-11c will be negative if x is taken horizontally and y vertically upwards. The boundary conditions are the no-slip conditions at the walls and bottom, the slip condition at the interface with no flow penetration, the adiabatic condition at the walls, heat flux input at the bottom caused by solar input, and conductive heat loss at the interface. If the governing equations are nondimensioned, the dimensionless parameters obtained are Re, Fr, aspect ratio D/L, and the Richardson number at the interface. The Richardson number must be greater than 0.85 to ensure negligible entrainment from the nonconvective zone and, thus, an undisturbed gradient layer.

For an experimental modeling of the energy extraction process, Re, Fr, and D/L must be simulated with $Ri \gtrsim 0.85$ at the interface. For the end-to-end extraction, $Fr' \gtrsim 1.0$ ensures entrainment into the entering flow and, thus, a rapid decay of buoyancy effects. Except for this, Fr is not critical to an experimental modeling of the end-to-end flow configuration. Thus, Re is the most important parameter and even a zero buoyancy defect ($Fr \to \infty$) circumstance would allow a satisfactory simulation of the actual conditions. With good mixing at the inlet, even D/L is not a very important parameter, as long as L is large enough to allow the mixing to be completed before outflow.

The top-to-bottom configuration is much more complicated. The Reynolds number characterizing full-scale solar ponds must be reproduced in the laboratory so that the flow pattern, turbulence level, etc., are simulated. However, for a fully turbulent flow, Re might only have to be large enough to obtain turbulent flow in the laboratory. Since a large penetration is desired, $Fr \lesssim 1.0$. This leads to a minimum value of ΔT for a given flow rate, which is itself determined by Re. Therefore, the zero buoyancy defect case is not of much value. The slot width and ΔT must be chosen so that $Fr \lesssim 1.0$, and since attempts will be made to achieve this condition in actual ponds, the flow rate and ΔT in the laboratory will have to be close to those under actual pond conditions.

Another parameter e, which may be termed the energy extraction parameter, is defined as:

$$e = E_{s1}/(\rho C_p Q \Delta T) \quad , \tag{3-9}$$

where E_{s1} is the solar energy absorbed in the storage layer. This parameter compares the energy put into the layer with that extracted from it. In actual ponds, e would be close to unity. In the laboratory, the extraction is close to that of an actual pond since Fr and Re are kept essentially the same. However, the total energy absorbed in the storage layer depends on the pond surface area. Since the heat flux per unit area is the same, the total energy in the laboratory is much less because of the much smaller surface area. Therefore, in the laboratory e generally will be much less than unity. This means that energy is extracted from a storage layer with almost no energy input and, therefore, a continuous operation is not possible. A constraint on the operating time exists and is determined by the time required when a significant temperature drop is observed at the outlet. Therefore, a transient problem has to be studied in the laboratory to simulate the continuous energy extraction from an actual solar pond.

Some work has been done on discharging warmer or colder water into initially isothermal water contained in a tank. Lavan and Thompson (1977) investigated energy extraction from a tank of hot water and studied the outflow temperature as a function of time. Figure 3-11 shows a typical variation obtained for the conditions indicated. The outflow temperature remains unaltered for about 6.5 min and then drops very sharply. This indicates that the cold fluid acts as a plug, causing the outflow temperature to drop rapidly as the cold front traveling upwards reaches the outflow port.

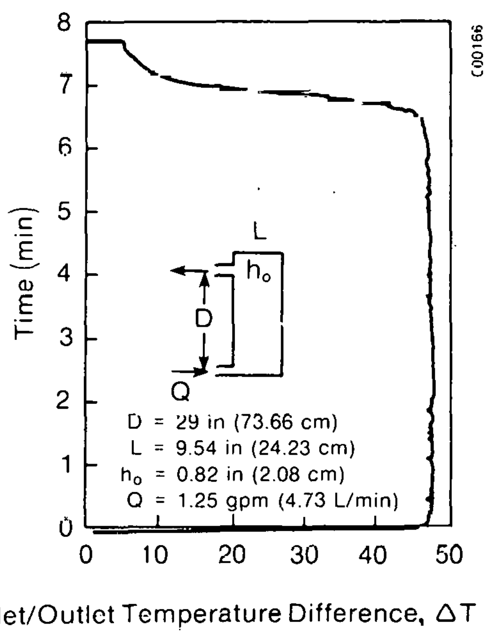

SOURCE: Lavan and Thompson 1977

Figure 3-11. Typical Trace of Exit Water Temperature

Gupta and Jaluria (1980) observed similar behavior for a thermal discharge at the top of the tank and an outflow at the bottom, as shown in Figs. 3-12 and 3-13. The outflow temperature remains unaltered up to a physical time of about 4 h. The flow rate for this experiment was 0.675×10^{-5} m^3/s, and the total volume of the water was 0.1548 m^3. If a plug flow is assumed, the time taken for the hot fluid to reach the bottom may be determined by employing the average vertical velocity as Q/A. Therefore, the time it takes for the heated fluid to traverse the depth D is given by:

$$t = D/(Q/A) = V_o/Q \quad , \tag{3-10}$$

where V_o is the volume of the water body and Q the flow rate. For Figs. 3-12 and 3-13, this time is estimated as 6.4 h. Therefore, the plug-flow model roughly estimates the time it takes the thermal effects to reach the outflow

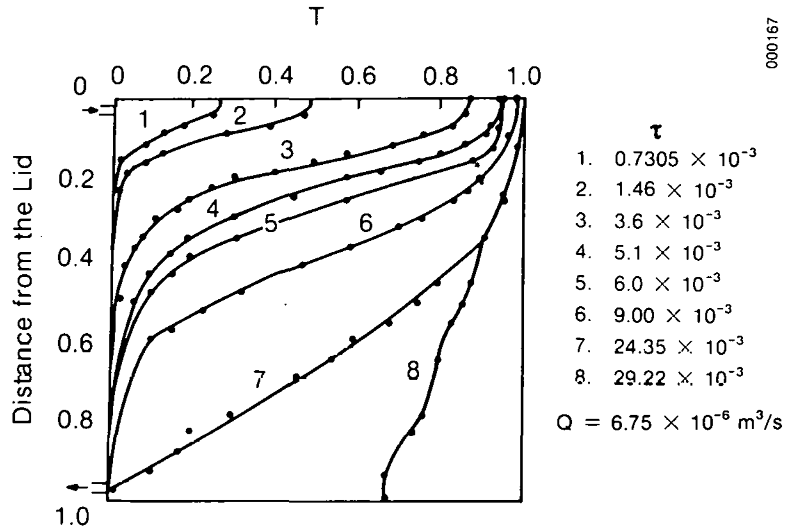

SOURCE: Gupta and Jaluria 1980

Figure 3-12. Transient Behavior of the Temperature Profiles with Inflow and Outflow Located at the Top and Bottom, Respectively

location. Repeating this process for the laboratory case, a time of 2.8 h is estimated for a flow of 10^{-3} m^3/s and a storage layer volume of 10 m^3. In view of the discrepancy between the estimated time (6.4 h) and the actual time shown in Fig. 3-13, a time of about 1.8 h may be expected in actual experimentation before a sharp temperature drop is observed at the outflow.

The time constraint arises because the energy extraction levels of a full-sized pond are being simulated in the laboratory to obtain the same Re and Fr; however, the energy input into the storage layer is much smaller in the laboratory because the area of the tank is much smaller. If a flow per unit width of 10^{-3} m^3/s-m in a 1-km^2 surface area pond is simulated, the extraction parameter e is ~0.01 for an actual pond 1 km long, whereas the laboratory facility is ~10 m in length. If, however, e is kept at 1.0 in the laboratory, the corresponding flow rate is 10^{-5} m^3/s-m. This makes the Froude number much less than 1.0 and, hence, avoids entrainment into the cold inflowing water. But it gives a much smaller Fr, one-hundredth the value for the full-scale pond conditions, which is more stable. The main problem, however, is that Re is ~20 in the laboratory and ~2000 for the continuous operation in the actual pond. Therefore, laboratory and pond flow are quite different.

The mixing effect and the disturbance to the interface would also not be modeled satisfactorily in the laboratory. It is possible to adjust the physical variables of the problem, particularly Q, ΔT, and h_0, to experimentally simulate actual pond conditions keeping the physical constraints satisfied. Thus Ri $\gtrsim$ 1.0 at the interface, Fr $\lesssim$ 1.0 at the inlet, and Re should be large enough to give a similar flow pattern.

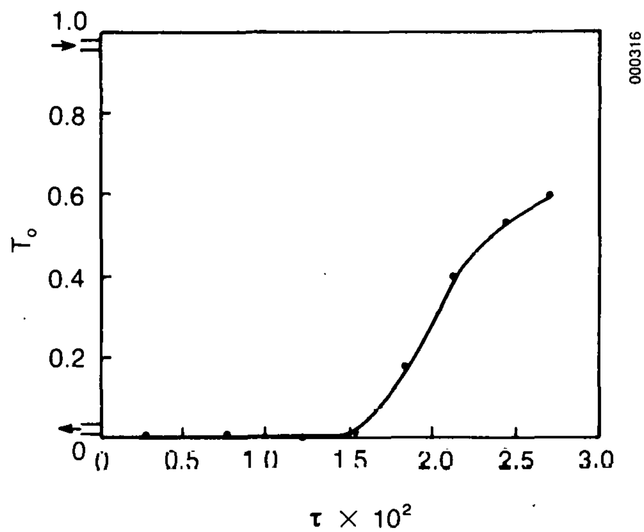

SOURCE: Gupta and Jaluria 1980

Figure 3-13. Outflow Temperature versus Time with Inflow and Outflow Located at the Top and Bottom, Respectively

For a flow of 10^{-5} m^3/s-m, the energy extraction parameter e is 1.0 and a continuous operation of the laboratory system is possible. Even if no energy input into the storage layer occurs, the plug-flow model gives an operation time of several days. Therefore, simulating the actual system by keeping Re and Fr the same leads to a time constraint. If e is kept as unity, the flow and thermal fields are only partially simulated. Oberkampf and Crow (1976) and Cabelli (1977) observe that the flow takes a long time to be fully established. In a very short time (minutes) the flow apparently establishes a pattern that changes very gradually because of the diffusion of thermal effects. Therefore, when operating with Re and Fr corresponding to the full pond conditions, one has to contend with gradually varying thermal and velocity fields. However, the experiments would indicate the level of mixing, the effect on the interface (at least for short-term peaking power circumstances), and the flow pattern that arises.

The aspect ratio D/L is also an important parameter in the top-to-bottom configuration. The flow pattern, recirculation, and flow penetration stongly depend on the aspect ratio; but it is extremely hard, if not impossible, to attain low aspect ratios in the laboratory. A full-scale solar pond may have an aspect ratio of 10^{-3} while in the laboratory it would be ~0.1. The depth of the storage layer cannot be scaled down to one-hundredth its value in actual ponds if the length is scaled down this far. Therefore, it becomes necessary to study various aspect ratios and determine the effect they would have on the flow. An extrapolation to the aspect ratio typical of a full-sized pond may then be possible.

From this discussion, it is apparent that an experimental modeling of the end-to-end configuration may be carried out quite satisfactorily as long as some of the essential constraints are satisfied, such as Ri $\gtrsim$ 1.0 at the interface. For the top-to-bottom configuraton, the question is more complicated, and a complete experimental modeling of the full-scale solar pond does not appear feasible. However, if the essential constraints are met, some flexibility in the choice of the governing parameters exists, and the basic aspects of the flow may be studied. In this case, it is important to add an analytical model to the experimental study to confidently predict the expected behavior in full-sized ponds. Table 3-1 lists some of the important results obtained in this preliminary study of energy extraction. Further analytical work may be undertaken after obtaining some experimental results.

Table 3-1. Summary of Results for Energy Extraction
(1-km^2 pond, $1\text{-m}^3/\text{s}$ flow from a 3-cm slot)

1. Interface is stable.
2. If Fr $\lesssim$ 1.0 penetration is ~300 m.
3. Top-to-bottom extraction is feasible for small ponds.
4. Inflow/outflow must be about 6 cm away from interface.
5. There is a time constraint for experimental study.
6. Flow establishment takes a few hours.
7. Basic parameters are Re, Fr, Ri, D/L.
8. End-to-end extraction may be studied with $\Delta T = 0$.
9. Experimental system simulates top-to-bottom extraction partially.

SERI

SECTION 4.0

CONCLUSIONS

The purpose of this study was to evaluate the effects heat rejection and energy extraction would have on the performance of the solar pond and to obtain preliminary data on the feasibility of top-to-bottom recirculating flow. This study was based on earlier studies mostly on heat rejection from power plants to water bodies, such as ponds and lakes, and on simplified models.

Considerable information exists on heat rejection from power plants to water bodies using a recirculating thermal discharge. Much of this information can be used with modifications for this study. The most relevant investigations are those concerned with the surface energy exchange, the surface jet flow, recirculation in enclosed regions, and the stability of and the flow in a stratified medium. The problems under consideration have received essentially no attention in the literature. But related experimental and numerical results may be used to predict the anticipated flow field and the thermal effects in the surface layer as well as in the storage zone.

For both problems, physical variables were used to determine the governing dimensionless parameters. On this basis, the stability of the nonconvecting gradient zone and the nature of the resulting flow was determined. An interesting result from the fundamental studies on flow in stratified media is the decrease in entrainment of ambient fluid in a flow with the Richardson number, which compares the gravitational effects with those caused by the flow. For $Ri > 0.85$, the flow does not entrain the ambient fluid, and the flow rate remains unchanged. This will also occur if $Fr \lesssim 1.0$ for linear variations in density and velocity. This is important since it means that the entering flow is not mixed with the ambient fluid leading to a much greater flow penetration.

The heat rejection problem was considered, including evaporation, radiation, and the flow that arises in the surface layer. A 3-MW power plant on a 1-km^2-surface area pond with a thermal-to-electric efficiency of 8% gives a heat rejection of 34.5 W/m^2 into the surface layer. Table 2-1 gives some of the results obtained for this value, which is typical of solar ponds in the western United States when considering a 24-hour yearly average of the incident solar flux. The average surface temperature rises by ~2°C, leading to an increase in evaporation that is ~1% of the flow rate, or ~17% of the natural evaporation. Evaporation and back radiation mainly cause the energy loss, which gives a surface heat transfer coefficient in the range 15-25 W/m^2 K. The exact value is determined by considering various energy exchange mechanisms. The interface with the gradient zone is quite stable if the diffusers are spread out to obtain a two-dimensional flow and are located near the surface. The outflow must be at least 400 m from the inflow, so that enough distance is provided for the input energy to be lost to the environment and the outflow temperature to remain unaltered. If Fr is maintained at <1.0 at the inlet, there is no entrainment for ~300 m from the inlet. This reduces the disturbance to the interface and allows the hot fluid to float at the surface losing energy to the atmosphere at a greater rate. The problem is time dependent because of the variation in the ambient conditions. It can be approached as a quasisteady problem, considering the conditions at various times during the year. A transient analysis is needed to study the variation from day to night.

For the energy extraction problem, two flow configurations were considered: top-to-bottom and end-to-end. Employing the earlier results on heat rejection, particularly on surface jets and flow in stratified media, the effect of the flow on the pond performance was studied. Table 3-1 shows the important results obtained for a two-dimensional flow of 10^{-3} m^3/s-m using a slot height of 3 cm. The gradient zone is undisturbed if a two-dimensional flow is maintained with the inflow/outflow ports about 6 cm away from the interface. Flow penetration of ~300 m is estimated for the top-to-bottom configuration. The end-to-end configuration may be satisfactorily modeled in the lab, but the top-to-bottom configuration cannot be completely modeled. A constraint on the operation time arises in the latter case, and a transient problem has to be studied to model the continuous extraction in actual ponds. Individual aspects of the flow may be studied by varying the governing parameters. A full-sized pond is needed to answer some important questions regarding this configuration, which SERI has only recently suggested as an alternative.

From the results obtained, one can see that heat rejection to the surface layer is feasible and the pond is not detrimentally affected if care is taken to keep the disturbance to the interface negligible. The top-to-bottom configuration appears feasible for small- to medium-sized ponds with a length less than 300 m. The end-to-end configuration is satisfactory for large ponds and can be satisfactorily modeled in the lab. The top-to-bottom configuration cannot be completely and uniquely modeled in the lab. Its individual aspects may be studied with further work carried on in full-scale ponds.

SECTION 5.0

RECOMMENDATIONS

This preliminary study has determined several very important considerations in heat rejection to the surface region and energy extraction from the storage zone of a salt-gradient solar pond. The results will provide guidelines for the design of the system particularly regarding the design and location of the withdrawal and injection ports. A two-dimensional flow employing several diffusers that spread out the flow at one end of the pond is desirable since it reduces the velocities considerably, which in turn reduces the disturbance to the gradient zone. The ports should be sufficiently high (3 cm for a flow of 10^{-3} m^3/s-m), to avoid mixing the flow at the inlet for the heat rejection and for the top-to-bottom energy extraction problems. For the end-to-end extraction, a good mixing at the entrance may be desirable and a smaller slot height would be suitable. The ports must be positioned as far as possible from the interface--at the surface for heat rejection and at least 6 cm from the interface for a flow of 10^{-3} m^3/s-m in energy extraction. One can determine a suitable distance for a given flow rate. Similarly, one can calculate the necessary distance between the inflow and outflow for heat rejection. For a heat rejection of 34.5 W/m^2, it is 400 m. The average surface temperature rise and the increase in evaporation caused by heat rejection must be determined for a given circumstance.

The end-to-end configuration is suitable for all ponds, while the top-to-bottom extraction appears satisfactory only for small to medium ponds less than 300-m long. However, for large ponds it is not necessary to go from one end to the other. Considerable savings in piping costs and heat loss can be achieved by locating the outflow port between the two ends and by determining the distance from the inlet using the two extreme flow configurations.

Laboratory experiments should be directed at verifying some of the important findings of this study, particularly concerning flow penetration and interface stability. The effect of the physical variables may be studied with the governing dimensionless parameters obtained here. Since the top-to-bottom configuration cannot be adequately modeled in the lab, the results should be coupled with an analytical model. The predictions of the analysis for the lab flow may be verified experimentally and the model extended to provide information for larger ponds. Some experimental work in full-scale ponds would also be needed to answer questions pertaining to flow penetration and to provide inputs to the analytical model. A numerical model for the two-dimensional flow that arises may be developed on the basis of the work done here.

Similarly, the energy exchange at the surface is difficult to model in the laboratory. Analysis may be employed, along with experimentation, to provide information for designing solar ponds and the related flow systems.

SERI

SECTION 6.0

REFERENCES

Abraham, G. 1965. "Horizontal Jets in Stagnant Fluid of Other Density." J. Hyd. Div. Vol. 91 (HY4): pp. 138-154.

Bejan, A. and Imberger, J. 1979. "Heat Transfer by Forced and Free Convection in a Horizontal Channel with Differentially Heated Ends." J. Heat Transfer. Vol. 101: pp. 417-421.

Bejan, A. and Tien, C. L. 1978. "Laminar Natural Convection Heat Transfer in a Horizontal Cavity with Different End Temperatures." J. Heat Transfer. Vol. 100: pp. 641-647.

Brocard, D. N. and Harleman, D. R. F. 1980. "Two-Layer Model for Shallow Horizontal Convective Circulation." J. Fluid Mech. Vol. 100: pp. 129-146.

Bryant, P. J. and Wood, I. R. 1976. "Selective Withdrawal from a Layered Fluid." J. Fluid Mech. Vol. 77: pp. 581-591.

Cabelli, A. 1977. "Storage Tanks--A Numerical Experiment." Solar Energy. Vol. 19: pp 45-54.

Crapper, P. F. and Linden, P. F. 1974. "The Structure of Turbulent Density Interfaces." J. Fluid Mech. Vol. 65: pp. 45-63.

Darden, R. B.; Imberger, J.; and Fischer, H. B. 1975. "Jet Discharge Into a Stratified Reservoir." J. Hyd. Div. Vol. 101 (HY9): pp. 1211-1220.

Debler, W. R. 1959. "Stratified Flow Into a Line Sink." J. Eng. Mech. Div. Vol. 85: pp: 51-65.

Edinger, J. E.; Duttweiler, D. W.; and Geyer, J. C. 1968. "The Response of Water Temperatures to Meteorological Conditions." Water Resources Res. Vol. 5: pp. 1137-1143.

Elata, C. and Levin, O. 1965. "Hydraulics of the Solar Pond." Proceedings of the 11th Congress of the International Association for Hydraulics Research. Leningrad, U.S.S.R.

Elata, C.; Levin, O.; and Hadar, A. 1962. "On Some Flow Problems of the Solar Pond." The Solar Pond Project. Report S/118/62 (in Hebrew). National Council for Research and Development of Israel.

Ellison, T. H. and Turner, J. S. 1959. "Turbulent Entrainment in Stratified Flows." J. Fluid Mech. Vol. 6: pp. 423-448.

Engelund, F. 1976. "Hydraulics of Surface Buoyant Jet." J. Hyd. Div. Vol. 102 (HY9): pp. 1315-1325.

Foster, T. D. 1971. "A Convective Model for the Diurnal Cycle in the Upper Ocean." J. Geophys. Res. Vol. 76: pp. 666-675.

Gupta, S. K. and Jaluria, Y. 1980. "Thermal Stratification in Water Storage System." ASME Paper No. 80-C2-Sol-6. Presented at the ASME Century 2 Solar Energy Conf., San Francisco, CA.

Gupta, S. K. and Jaluria, Y. 1981. "Transient Thermal Effects in an Enclosed Water Body Due to Heated Water Discharge for Heat Rejection and Solar Energy Storage." Energy Conv. and Mgmt. Vol. 21: pp. 3-8.

Harris, M. J., and Wittenberg, L. J. 1979. "Heat Extraction from a Large Salt Gradient Solar Pond." Report TP-245-430. Proceedings of the Solar Heating and Cooling Systems Conference--Operational Results. Held in Colorado Springs, CO, 27-30 November 1979. Golden, CO: Solar Energy Research Institute.

Hindley, R. D. and Miner, R. M. 1972. "Evaluating Water Surface Heat Exchange Coefficient." J. Hyd. Div. Vol. 98 (HY8): pp. 1411-1426.

Imberger, J. 1972. "Two-Dimensional Sink Flow of a Stratified Fluid Contained in a Duct." J. Fluid Mech. Vol. 53: pp. 329-349.

Imberger, J. and Fandry, C. 1975. "Withdrawal of a Stratified Fluid from a Vertical Two-Dimensional Duct." J. Fluid Mech. Vol. 70; pp. 321-332.

Imberger, J., Thompson, R., and Fandry, C. 1976. "Selective Withdrawal from a Finite Rectangular Tank." J. Fluid Mech. Vol. 78: pp. 489-512.

Jaluria, Y. 1979. "Thermal Effects of Energy Discharge to a Lake." Proceedings of the International Conference on Num. Meth. Thermal Problems. Swansea, United Kingdom. July 1979.

Jaluria, Y. 1980. Natural Convection Heat and Mass Transfer. Oxford, England: Pergamon Press.

Jaluria, Y. and Gupta, S. K. 1980. "A Numerical Study of Mixed Convection Flow in Enclosures." Proceedings of the ASME 19th National Heat Transfer Conference, ASME Paper No. 80-HT-80. ,FL.

Jen, Y.; Wiegel, R. L.; Mobarek, L. 1966. "Surface Discharge of Horizontal Warm Water Jet." J. Power Div. Vol. 92: pp. 1-30.

Jirka, G. H.; Abraham, G.; Harleman, D. R. F. 1975. An Assessment of Techniques for Hydro Thermal Prediction. Report No. B 250509. Available through NTIS. U.S.A.

Kao, T. W. 1963. The Phenomenon of Blocking in Stratified Flows. Ph.D. thesis. , MI: University of Michigan.

Kao, T. W. 1965. "A Free-Streamline Solution for Stratified Flow into a Line Sink." J. Fluid Mech. Vol. 21: pp. 535-543.

Kao, T. W. 1976. "Selective Withdrawal Criteria of Stratified Fluids." J. Hyd. Div. Vol. 102 (HY6): pp. 717-729.

Kaufman, D. W. 1960. Sodium Chloride. Washington, DC: American Chemical Society, Chapter 25.

Koh, R. C. Y. 1966. "Viscous Stratified Flow Towards a Sink." J. Fluid Mech. Vol. 24: pp. 555-575.

Koh, R. C. Y. 1971. "Two-Dimensional Surface Warm Jets." J. Hyd. Div. Vol. 97 (HY6): pp 319-836.

Lavan, Z. and Thompson, J. 1977. "Experimental Study of Thermally Stratified Hot Water Storage Tanks." Solar Energy. Vol. 19: pp. 519-524.

List, E. J. and Imberger, J. 1973. "Turbulent Entrainment in Buoyant Jets and Plumes." J. Hyd. Div. Vol. 99: (HY9): pp. 1461-1474.

Lofquist, K. 1960. "Flow and Stress Near an Interface Between Stratified Liquids." Phys. Liquids. Vol. 3: pp. 158-175.

McGuirk, J. J. and Rodi, W. 1979. "Mathematical Modeling of Three-Dimensional Heated Surface Jets." J. Fluid Mech. Vol. 95: pp. 609-633.

Miles, J. W. 1961. "On the Stability of Heterogeneous Shear Flows." J. Fluid Mech. Vol. 10: pp. 496-508.

Mitry, A. M. and Ozisik, M. N. 1976. "A One-Dimensional Model for Seasonal Variation of Temperature Distribution in Stratified Lakes." Int. J. Heat Mass Transfer. Vol. 19: pp. 201-205.

Miyazaki, H. 1974. "Heated Two-dimensional Jet Discharged at Water Surface." Int. J. Heat Mass Transfer. Vol. 17: pp. 1269-1272.

Moore, F. K. and Jaluria, Y. 1972. "Thermal Effects of Power Plants on Lakes." J. Heat Transfer. Vol. 94: pp. 163-168.

Moore, M. J. and Long, R. L. 1971. "An Experimental Investigation of Turbulent Shearing Flow." J. Fluid Mech. Vol. 49: pp. 635-655.

Morton, B. R. 1959. "Forced Plumes." J. Fluid Mech. Vol. 5: pp. 151-163.

Nielsen, C. E. 1976. "Experience with a Prototype Solar Pond for Space Heating." Sharing the Sun: Solar Technologies in the Seventies. Vol 5: pp. 169-182. Proceedings of the 1976 AS/ISES Conference, Winnipeg, Canada, 15-20 August.

Nielsen, C. E. 1979. "Nonconvective Salt Gradient Solar Ponds." Solar Energy Handbook. Edited by W. C. Dickinson and P. M. Cheremisinoff. New York, NY: Marcel Dekker, Inc.

Noble, R. D. 1981. "Comparison of Two Surface Heat Exchange Models." J. Hyd. Div. Vol. 107 (HY3): pp. 361-366.

Office of Saline Water. 1971. Saline Water Conversion Engineering Data Book. Washington, DC: U.S. Department of the Interior. pp. 12.00-12.95.

Oberkampf, W. F. and Crow, L. I. 1976. "Numerical Study of the Velocity and Temperature Fields in a Flow Through a Reservoir." J. Heat Transfer. Vol. 98: pp. 353-359.

Pao, H. P. and Kao, T. W. 1974. "Dynamics of Establishment of Selective Withdrawal of a Stratified Fluid from a Line Sink." Parts 1 and 2. J. Fluid Mech. Vol. 65: pp. 657-710.

Park, G. G. and Schmidt, P. S. 1973. "Numerical Modeling of Thermal Stratification in a Reservoir with Large Discharge to Volume Ratio." Water Resources Bulletin. Vol. 9: pp. 932-941.

Raphael, J. M. 1962. "Prediction of Temperature in Rivers and Reservoirs." J. Power Div. Vol. 88: pp 157-181.

Riester, J. B.; Bajura, R. A.; Schwartz, S. H. 1980. "Effects of Water Temperature and Salt Concentration on the Characteristics of Horizontal Buoyant Submerged Jets." J. Heat Transfer. Vol. 102: pp. 557-562.

Ryan, P. J.; Harleman, D. R. F.; and Stolzenbach, K. D. 1974. "Surface Heat Loss from Cooling Ponds." Water Resources Res. Vol. 10: pp. 930-938.

Sehgal, R. C. and Jaluria, Y. 1979. "On the Horizontal Recirculation in Water Bodies Due to Thermal Discharge." Proceedings of the 18th National Heat Transfer Conference. ASME Paper No. 79-HT-84.

Shah, M. M. 1981. "Estimate of Evaporation from Horizontal Surfaces." ASHRAE Trans. Paper No. 2612. Vol. 87 (No. 1).

Sliwinski, B. J. 1980. Investigation of Methods to Predict Thermal Stratification and Its Effect on Solar Energy System Performance. Rep. No. CERL-SR-E-160. Available through NTIS, U.S.A.

Spalding, D. B. 1977. "Heat and Mass Transfer in Rivers, Bays, Lakes and Estuaries." Adv. Heat Transfer. Vol. 13: pp. 61-117. , NY: Academic Press.

Stolzenbach, K. D. and Harleman, D. R. F. 1973. "Three-Dimensional Heated Surface Jets." Water Resources Res. Vol. 9: pp. 129-137.

Tabor, H. 1980. "Nonconvecting Solar Ponds." Phil. Trans. Royal Soc. London, England; A295; pp. 423-433.

Tamai, N.; Wiegel, R. L.; and Tornberg, G. F. 1969. "Horizontal Surface Discharge of Warm Water Jets." J. Power Div. Vol. 95: pp. 253-276.

Turner, J. S. 1965. "The Coupled Turbulent Transports of Salt and Heat Across a Sharp Density Interface." Int. J. Heat Mass Transfer. Vol. 8: pp. 759-767.

Turner, J. S. 1973a. "The Influence of Molecular Diffusivity on Turbulent Entrainment Across a Density Interface." J. Fluid Mech. Vol. 33: pp. 639-656.

Turner, J. S. 1973b. Buoyancy Effects in Fluids. United Kingdom: Cambridge University Press.

Wada, A. 1967a. "Study on Recirculation of Cooling Water of Power Station Sited on a Bay." Coastal Eng. Japan; Vol. 10: pp. 143-170.

Wada, A. 1967b. "A Study on Phenomena of Flow and Thermal Diffusion Caused by Outfall Cooling Water." Proceedings of the 10th Conference Coastal Eng. Vol. 2: pp. 1389-1411.

Wada, A. 1968c. "Studies on Prediction of Recirculation of Cooling Water in a Bay." Proceedings of the 11th Conference Coastal Eng. London, England; pp. 1453-1471.

Wada, A. 1968b. "Numerical Analysis of Distribution of Flow and Thermal Diffusion Caused by Outfall of Cooling Water." Coastal Eng. Japan; Vol. 11: pp. 161.

Wada, A. 1969. "A Study of Mixing Process in the Sea Caused by Outfall of Industrial Waste Water." Coastal Eng. Japan; Vol. 12: pp. 147-158.

Wiuff, R. 1978. "Experiments on Surface Buoyant Jet." J. Hyd. Div. Vol. 104 (HY5): pp. 667-679.

Wood, I. R. 1968. "Selective Withdrawal from a Stably Stratified Fluid." J. Fluid Mech. Vol. 32: pp. 209-223.

Yih, C. S. 1958. "On the Flow of a Stratified Fluid." Proceedings of the 3rd National Conference Appl. Mech. pp. 857-861.

Yih, C. S. 1960. "Exact Solutions for Steady Two-Dimensional Flow of a Stratified Fluid." J. Fluid Mech. Vol. 9: pp. 161-174.

Yih, C. S. 1980. Stratified Flows. Academic Press.

Zangrando, F. and Bryant, H. C. 1977. "Heat Extraction from a Salt Gradient Solar Pond." Proceedings of the Int. Conf. on Alt. Energy Sources. Vol. 6: pp. 2935-2967. Miami Beach, FL; 5-7 Dec.; Hemisphere Pub.

Zangrando, F. 1979. Observations and Analysis of a Full-Scale Experimental Salt Gradient Solar Pond. Ph.D. Thesis. Albuquerque, NM: Dept. of Physics and Astronomy, University of New Mexico.

Document Control Page	1. SERI Report No. SERI/RR-252-1393	2. NTIS Accession No.	3. Recipient's Accession No.

4. Title and Subtitle Heat Rejection and Energy Extraction Within Solar Ponds	5. Publication Date February 1982 6.
7. Author(s) Yogesh Jaluria	8. Performing Organization Rept. No.
9. Performing Organization Name and Address Solar Energy Research Institute 1617 Cole Boulevard Golden, Colorado 80401	10. Project/Task/Work Unit No. 2700.37 11. Contract (C) or Grant (G) No. (C) (G)
12. Sponsoring Organization Name and Address	13. Type of Report & Period Covered Research Report 14.

15. Supplementary Notes

16. Abstract (Limit: 200 words)

A study of the heat transfer and fluid flow processes governing heat rejection to the surface layer and energy extraction from the storage zone has been carried out. The literature available on this and other related problems was studied in detail to determine the nature of the recirculating flows that arise and the effect they might have on the stability of the gradient layer. Simplified analytical models were considered to determine the governing parameters and their effect on the performance and efficiency of the solar pond. Estimates of the surface temperature rise and the increase in evaporation caused by heat rejection were made. Two flow configurations, end-to-end and top-to-bottom, were considered for every extraction and the spread of the flow in the storage zone was studied. It was found that the limited penetration of the top-to-bottom configuration restricts its satisfactory operation to small ponds. The experimental modeling of the flows under study was considered in terms of the governing parameters and it was found that the top-to-bottom configuration cannot be uniquely modeled. The choice of these parameters for a full-size pond is also discussed.

17. Document Analysis

a. Descriptors Performance; solar ponds; salinity gradients; salinity gradient power plants; solar power plants; heat extraction; energy losses; fluid flow; heat transfer; design

b. Identifiers/Open-Ended Terms

c. UC Categories 59c,62

18. Availability Statement National Technical Information Service U.S. Department of Commerce 5285 Port Royal Road Springfield, Virginia 22161	19. No. of Pages 57 20. Price $5.25

Form No. 8200-13 (6-79)

☆ U.S. GOVERNMENT PRINTING OFFICE: 1982—577-952/164 Region No. 8.